

Visualization of Flows in Packed Beds of Twisted Tapes

R.C. Hendricks
Glenn Research Center, Cleveland, Ohio

M.J. Braun and D. Peloso
University of Akron, Akron, Ohio

M.M. Athavale
CFD Research Corporation, Huntsville, Alabama

R.L. Mullen
Case Western Reserve University, Cleveland, Ohio

The NASA STI Program Office . . . in Profile

Since its founding, NASA has been dedicated to the advancement of aeronautics and space science. The NASA Scientific and Technical Information (STI) Program Office plays a key part in helping NASA maintain this important role.

The NASA STI Program Office is operated by Langley Research Center, the Lead Center for NASA's scientific and technical information. The NASA STI Program Office provides access to the NASA STI Database, the largest collection of aeronautical and space science STI in the world. The Program Office is also NASA's institutional mechanism for disseminating the results of its research and development activities. These results are published by NASA in the NASA STI Report Series, which includes the following report types:

- **CONFERENCE PUBLICATION.** Collected papers from scientific and technical conferences, symposia, seminars, or other meetings sponsored or cosponsored by NASA.
 - **SPECIAL PUBLICATION.** Scientific, technical, or historical information from NASA programs, projects, and missions, often concerned with subjects having substantial public interest.
 - **TECHNICAL TRANSLATION.** English-language translations of foreign scientific and technical material pertinent to NASA's mission.
- Specialized services that complement the STI Program Office's diverse offerings include creating custom thesauri, building customized databases, organizing and publishing research results . . . even providing videos.
- For more information about the NASA STI Program Office, see the following:
- Access the NASA STI Program Home Page at <http://www.sti.nasa.gov>
 - E-mail your question via the Internet to help@sti.nasa.gov
 - Fax your question to the NASA Access Help Desk at 301-621-0134
 - Telephone the NASA Access Help Desk at 301-621-0390
 - Write to:
NASA Access Help Desk
NASA Center for AeroSpace Information
7121 Standard Drive
Hanover, MD 21076



Visualization of Flows in Packed Beds of Twisted Tapes

R.C. Hendricks
Glenn Research Center, Cleveland, Ohio

M.J. Braun and D. Peloso
University of Akron, Akron, Ohio

M.M. Athavale
CFD Research Corporation, Huntsville, Alabama

R.L. Mullen
Case Western Reserve University, Cleveland, Ohio

Prepared for the
Second Pacific Symposium on Flow Visualization and Image Processing
sponsored by the Pacific Center of Thermal-Fluids Engineering
Honolulu, Hawaii, May 16–19, 1999

National Aeronautics and
Space Administration

Glenn Research Center

Available from

NASA Center for Aerospace Information
7121 Standard Drive
Hanover, MD 21076

National Technical Information Service
5285 Port Royal Road
Springfield, VA 22100

Available electronically at <http://gltrs.grc.nasa.gov>

VISUALIZATION OF FLOWS IN PACKED BEDS OF TWISTED TAPES

R.C. Hendricks

National Aeronautics and Space Administration
Glenn Research Center
Cleveland, Ohio 44135

M.J. Braun and D. Peloso
University of Akron
Akron, Ohio 44325

M.M. Athavale
CFD Research Corporation
Huntsville, Alabama 35805

R.L. Mullen
Case Western Reserve University
Cleveland, Ohio 44106

INTRODUCTION

Although similar visualization materials and techniques have been discussed in previous work by Hendricks et al. (1997), we realized that printed frames, grabbed from videotapes of the flows in beds of packed spheres, failed to reproduce what was visualized. Herein we describe the events associated with packed beds of twisted tapes, but to fully appreciate the complexity of the flow fields, it becomes necessary to watch the videotape recording. However, the Full Flow Field Tracking (FFFT) method (Braun et al., 1988) can be applied to visualize and quantize the flow patterns and fluid velocities within a packed bed or a porous medium.

Packed beds of twisted tapes may serve as an alternative to porous-media packed beds in heat pipe applications in low- and high-body force fields, such as in space and gas turbine applications. Potentially, twisted tapes could also function as reaction surfaces where uniformity of mixing is sought. In this study the test section assembly simulated a canister of twisted tapes for heat, mass, and reaction exchange. An assembled cylinder would contain 6 to 10 such canisters in series. In turn, several cylinders would be bundled into an array. We tested only one simulated canister, although for any practical application simulation of an entire cylinder and array would be necessary. Power developed along the path and heat transfer and pressure drops downstream would modify the flows in the upstream leading canister even to the point of choking the element. Choking is quite serious because the power generation in a practical system is nearly constant and failure of the element becomes imminent.

ANALYSIS

Using twisted tapes (fig. 1, from Smithberg and Landis, 1964) is a well-known method for augmenting heat transfer in tubes at the expense of pressure drop in single-phase flows (Hong and Bergles, 1976; Lopina and Bergles, 1969; Bergles, 1998). Yet at constant pump power, twisted-tape, swirl-flow heat transfer can be increased by 20% over that of a straight tube (Lopina and Bergles, 1969). We will use these references as the starting point for representing the ideal packed bed of N twisted tapes (cf figs. 1 and 2) and work toward a porous-media model. The details are presented in appendix A.

For a single twisted tape in a tube the tangential fluid velocity is usually assumed to be linear with radial position (rotating slug flow) or

$$v_\theta = \frac{2\pi Ur}{H_o} \quad (1)$$

$$v_t = \frac{\pi U D}{H_o} \quad (2)$$

where r is the radial position, D is the twisted-tape diameter, H_o is the twist through 360° (one full wave), and U is the bulk average axial velocity. (All symbols are defined in appendix B.)

$$U = \frac{W}{\left(\frac{\pi D^2}{4} - wt \right) \rho} \quad (3)$$

where W is the mass flow rate, ρ is the average fluid bulk density, t is the tape thickness, and w is the tape width, and for $t \ll D$, $wt \rightarrow Dt$.

Single Twisted Tape in Tube

From figure 2 of Smithberg and Landis (1964), the data closely follow equation (1), except at the wall and centerline where $v_\theta = 0$, and nearly fit the following form:

$$\frac{v_\theta}{U} = C_o \left[1 - \left(\frac{r}{r_o} \right)^{27} \right] \frac{r}{r_o} \quad (4)$$

which is a close approximation to equation (1). For these data,¹ $Re_D = 137\,000$, $H_o/D = 3.62$, $D = 3.51$ cm (1.382 in.), and $v_{\theta,\text{exp}} = 71.63$ m/s (235 ft/s) at $r = 1.65$ cm (0.65 in.). At that point $r/r_o = 0.94$, $v_\theta = \pi(2r/D)(D/H_o)U$, or $U = 82.3$ m/s (270 ft/s). From equation (4)

$$C_o = \frac{\frac{235}{270}}{0.763} = 1.14 \quad (5)$$

Here $v_\theta \rightarrow U$ and even for this case neither an effective velocity (eq. (6) with $C_o = C_e$) nor an effective flow path (eq. (A12b)) is sufficient to account for the measured pressure drop increase in terms of f/f_o .

For laminar flows with Reynolds numbers less than 150, Date (1974) determined that D/H_o corrections are not required. However, for $150 < Re < 2000$ (and for turbulent flows), D/H_o corrections are necessary. From the f/f_o data of Smithberg and Landis (1964), $C_e \rightarrow 3$ with an equivalent velocity defined by using equation (2),

$$\frac{U_e}{U} = \left[1 + \left(\frac{C_e v_t}{U} \right)^2 \right]^{0.5} = \left[1 + \left(3\pi \frac{D}{H_o} \right)^2 \right]^{0.5} \quad (6)$$

The simple empirical form (eq. (6)) tends to group the turbulent friction data of Smithberg and Landis (1964) at a higher Reynolds number and identifies $(D/H_o)^2$ as a significant parameter for the analysis. However, there are additional Reynolds number and surface roughness dependencies (Gambill and Bundy, 1962). For example, at

¹The data point $Re_D = 137\,000$ with $D/D_H = 1.716$ becomes $Re_{D_H} = 79\,837$. Extrapolating the $H_o/D = 3.62$ locus may give $f/f_o = 2.8$, and this ratio may also be affected by roughness.

$\text{Re} = 25\,000$ the agreement of friction factors is good at high H_o/D , but at $\text{Re} = 6000$ the agreement is better at low H_o/D but is still not that good. The surface roughness is not given and is assumed to be that of a commercial tube.

Gambill and Bundy (1962) correlate the isothermal, single-twisted-tape data of several investigators with different surface roughness δ/D_e factors.

$$(f_s - f_a)_{e\text{iso}} = \left(\frac{0.21}{y^{1.31}} \right) \left(\frac{\text{Re}_e}{2000} \right)^{-n} \quad (\text{A43})$$

where

$$n = 0.81 \exp \left[-1700 \left(\frac{\delta}{D_e} \right) \right] \quad (\text{A43a})$$

$$f_a = 4f_o = \left(\frac{-dp}{dx} \right) \left(\frac{D_e}{0.5\rho U^2} \right) \quad (\text{A43b})$$

and y is the number of tube diameters per 180° of twist ($y = H/D$ or $2y = H_o/D$).

$H_o/D = 2y$	$\delta/D_e = 0$			$\delta/D_e = 0.00005$			$\delta/D_e = 0.0005$		
	6000	25 000	80 000	6000	25 000	80 000	6000	25 000	80 000
	$f_a = 4f_o = 4(0.046/\text{Re}^{0.2}) : f_s$ from equation (A43)								
22	1.12	1.05	1.02	1.12	1.06	1.03	1.19	1.16	1.13
10.3	1.31	1.13	1.06	1.34	1.15	1.08	1.52	1.42	1.36
4.34	1.97	1.41	1.20	2.04	1.48	1.25	2.61	2.31	2.10
3.62	2.23	1.51	1.25	2.32	1.61	1.32	3.04	2.66	2.40

Packed Bed of Twisted Tapes

In the packed-bed experiment described herein the tapes were not bounded by tube walls. They were assembled into a uniform matrix of twisted tapes with the same twist direction, twist-to-diameter ratio H/D_o , and thickness t . The boundary conditions changed from those of a single twisted tape. The tangential velocity became zero at the center of the twisted tape and at the tangent points of the packed bed of virtual tubes of diameter D_o because the velocity fields were counterrotating. The rotating velocity external to the confines of the virtual cylinders was assumed to be small, thus permitting a local region of axial flow. As noted earlier, corrections for H/D_o effects in low-Reynolds-number flows are not required (Date, 1974). For $H/D_o > 3.6$ and $w \rightarrow D$, the tape lengths before and after the twist do not differ substantially.

In packed beds the superficial velocity is related to the bed porosity by

$$u = \frac{U_o}{\varepsilon} \quad (7)$$

where U_o is the empty or unpacked bed velocity and ε is related to the bed volume V as

$$\varepsilon = 1 - \frac{V_{\text{solid}}}{V_{\text{total}}} \quad (8)$$

For the present case each of 48 twisted tapes was considered as encased in a virtual tube, where the tape width $w = 0.3234$ cm (0.1273 in.) and the tape thickness $t = 0.1275$ cm (0.0502 in.).

$$D_o = \left(w^2 + t^2 \right)^{0.5} \quad (\text{A4})$$

Thus, $D_o = 0.348$ cm (0.137 in.) and $H_o = 5.503$ cm (2.17 in.). For this geometry $H_o/D_o = 15.8 \rightarrow H/D_o = 7.9$, or three 360° twists in 16.5 cm (6.5 in.).

For the packed bed of 48 twisted tapes considered herein, the orientation of the twist angle was somewhat irregular (figs. 2(b), (d), (e), and (f)); however, by using the prior relation for porosity and variations in t and w , the estimated porosity range becomes (see measurements and estimates in appendix A)

$$0.59 < \varepsilon < 0.63 \quad (9)$$

with a mass flow range of

$$1.6 < \frac{upA_o}{W} < 1.7 \quad (10)$$

where A_o is the cross section of the empty tube.

Parameters for Single Twisted Tape in Tube

The analysis and data of Smithberg and Landis (1964) were considered to provide insights into the effects of twist H/D or H/D_o and pressure drop. Reformulating the Ergun parameter Y_{Ergun} (Ergun, 1952) in terms of the Fanning friction factor (see appendix A) gives

$$f_{\text{Smithberg-Landis}} = \frac{1}{3} Y_{\text{Ergun}} \quad (\text{A14})$$

$$Y_{\text{Ergun}} = \left(\frac{\rho \Delta P}{G_o^2} \right) \left(\frac{\varepsilon^3}{1-\varepsilon} \right) \left(\frac{D_p}{L_o} \right) \quad (\text{A16})$$

where

$$G_o = \rho U_o \quad (\text{A15})$$

At high Reynolds numbers

$$Y_{\text{Ergun}} \rightarrow \text{Constant} \rightarrow 0.014 \quad \text{for } \varepsilon \rightarrow 1 \text{ and } \text{Re} \gg 2000 \quad (\text{A25})$$

where 0.014 is the commercial rough-tube equivalent. In equation (A16), L_o represents the straight-line distance between pressure taps. The twisted-tape length L varies little from L_o over the practical range of tapes. For laminar flows the correlated pressure drops are weakly dependent on twist H/D or H_o/D , yet for turbulent flows the pressure drop data are strongly dependent on twist. In most cases $dp/dz \rightarrow \Delta P/L$ for single tapes in tubes. So in terms of Reynolds number the packed-bed Reynolds parameter X_{Ergun} becomes

$$\text{Re}_{\text{Smithberg-Landis}} = \frac{2\varepsilon}{3} \left[\frac{G_o D_p}{(1-\varepsilon)\mu} \right] = \frac{2\varepsilon}{3} X_{\text{Ergun}} \quad (\text{A17})$$

where

$$X_{\text{Ergun}} = \frac{G_o D_p}{(1-\varepsilon)\mu} \quad (\text{A18})$$

$$(f \text{Re})_{\text{Smithberg-Landis}} = \frac{2\varepsilon}{9} Y_{\text{Ergun}} X_{\text{Ergun}} \quad (\text{A19})$$

and the generalized relation can be expressed as

$$X_{\text{Ergun}} Y_{\text{Ergun}} = 70.9 + \left[g_2 \left(\frac{H}{D}, k_s \right) \right] X_{\text{Ergun}} \quad (\text{A83})$$

From extrapolating the data $g_2(H/D, k_s) \rightarrow 0.014$ and represents a lower bound of the data as illustrated in figure 3 and labeled “single twisted tape.” To illustrate the dependency of the turbulent flow data on H_o/D , we normalized the Ergun friction factor by using equation (6). The modified Ergun friction factor is shown in figure 4 as

$$\left(Y_{\text{Ergun}} \right)_{\text{modified}} = \frac{Y_{\text{Ergun}}}{\left[1 + \left(3\pi \frac{D}{H_o} \right)^2 \right]^{0.5}} \quad (\text{11})$$

and tends to follow the simplified form

$$X_{\text{Ergun}} Y_{\text{Ergun}} = 70.9 + 0.014 X_{\text{Ergun}} \quad (\text{A83a})$$

TEST FACILITY

The test facility consisted of an oil tunnel, flow system components, video equipment, a laser, lens systems, data recorders, and a test configuration (fig. 5). The test section consisted of 48 twisted (spiral) Lucite tapes assembled into a bundle and placed into a clear Lucite tube 2.54 cm (1 in.) in diameter. The tape bundle simulated, for example, a system of catalytic reactive surfaces, heat transfer augmentation surfaces, or flows through strata of porous media. The twisted tapes were made from clear, polished Lucite sheet 0.152 cm (0.06 in.) thick cut into strips 0.318 cm (0.125 in.) wide by 17.8 cm (7 in.) long (nominal dimensions; measurements are discussed in appendix A). These strips were gripped 0.635 cm (1/4 in.) from each end and twisted with three complete twists (figs. 2(a), (d), and (f)). Figure 2(b) is a cross section of the actual packed bed, and figure 2(c) illustrates an ideal packed bed. A flow screen with 0.08-cm- (0.032-in.-) square mesh made of 0.023-cm- (0.009-in.-) diameter wire was placed across the tube inlet and attached to a square support (figs. 2(d) and (e)). For Borda inlet flows the screen restrained the axial movement of the twisted tapes and served as a screened orifice inlet when the test section was reversed. In the latter case, the twisted tapes were restrained 0.95 cm (0.375 in.) downstream by the visualization mirror. Some movement of the packed bed was noted. The movement would slightly disturb the inlet and exit flows but was not expected to alter the developed flow field.

The assembly (fig. 2(d)) was then placed into a closed-cycle oil tunnel (fig. 5) with a square support fabricated to retain the tube in the flow field and block the remaining tunnel cross section (152.4 cm by 7.62 cm by 7.62 cm; 60 in. by 3 in. by 3 in.). Both the upper wall and the viewing port walls of the tunnel were Lucite (fig. 5). The index of refraction of the oil matched that of the Lucite, and magnesium oxide particles were used as flow tracers. The flow field was visualized by using the Full Flow Field Tracking (FFFT) method (Braun et al., 1988). Laser light sheets illuminated two-dimensional sections of the tunnel along the flow path. Transverse visualization was accomplished by placing a mirror in the tunnel downstream of the 48-twisted-tape bundle and at approximately 45° to the flow axis. A second mirror placed above the tunnel (not shown in fig. 5) projected the view to the television camera. Cross tunnel traverses were accomplished by small rotations of the mirrors. These traverses provided insights into the three-dimensional nature of the flow field.

The coherent-beam, continuous-wave, argon-ion laser was directed by micrometric adjustable mirrors through two cylindrical lenses positioned at 90° to each other and through the Lucite tunnel window and into the test section. The light sheet was approximately 0.01 cm (0.004 in.) thick, and the flow was seeded with magnesium oxide flow tracers. Micrometric adjustments controlled scanning of the light slices across the test section and provided a three-dimensional visualization of the flow field, which was videotaped at 30 Hz.

EXPERIMENTAL RESULTS

Visualization

Figure 6 represents the axial flow field along the centerline of the packed bed of twisted tapes. Flows across the inlet were markedly influenced by the twist and packing of the bed. At the inlet the vena contracta normally found at the inlet of an open tube was limited to a minor region near the tube wall entrance (fig. 6(a)). Beyond this entrance region the flow was rapidly entrained into minor spiral perturbations ($H_o/D_o = 15.8$) within less than $0.1D$. However, for flows near adjacent solid boundaries there is clear evidence of local spiral flows within the field of focus. Flows in the boundary layer of each twisted tape tended to spiral as expected (fig. 6(b)). Thus, the flows tended to follow typical boundary layer flow patterns: no slip at the surface and a region of viscous flow closely aligned with the surface topology blending into a region of fully developed flows with minor perturbation of the streamlines. As the pressure drop was increased, these regions became less distinct in that the boundary layers became thin and difficult to visualize. There still persisted a region perturbed by the spiral nature of the surface, but it became less distinct as the flow velocity increased.

By aligning the laser sheet transverse to the flow we obtained a circular cross section of the flow. The packed bed of twisted tapes appeared as small, randomly oriented, rectangular blocks in the flow field (fig. 2(b)). There appeared regions where the flows were jetting between adjacent blocks, regions where the flows were predominantly clockwise or counterclockwise, regions where the flows were upward or downward, and wall boundary layer flows at both the “block” surfaces and the interfaces between the tube and the twisted tapes (fig. 7). Notably absent were local vortex flows, with the possible exception of one configuration. Although jetting should produce vortices, the three-dimensionality of the flow may have precluded observation. It appeared that engendered vorticity was captured within the axial spiral flow field, although not readily visualized.

Packed Bed of Twisted Tapes

The pressure drop and flow data parameters in table 1 were plotted in figure 8. The errors in the difference in static pressures upstream and downstream increased at lower Reynolds numbers, and those data should be considered suspect. It is evident that the Borda inlet configuration with a screen had a slightly higher flow resistance than the orifice configuration with a screen and that the orifice configuration without a screen had the lowest resistance. Consistent sets of parallel lines could be passed through each set of data in figure 8. Shown for reference are the Ergun (1952) porous-media model and the Date (1974) single-twisted-tape model. In general, the data were lower than the Ergun model over the range of data taken. The average fluid temperature was 22 ± 1 °C, the viscosity was 0.91 poise, and the density was 0.9 g/cm^3 . A suggested general form for N twisted tapes in a tube, following equation (A83), is

$$X_{\text{Ergun}} Y_{\text{Ergun}} = 45 + 0.009 X_{\text{Ergun}} \quad (\text{A83a})$$

which is considerably below that suggested for flows in porous media

$$X_{\text{Ergun}} Y_{\text{Ergun}} = 150 + 1.75 X_{\text{Ergun}} \quad (\text{A84})$$

suggesting significantly less flow resistance for the packed bed of twisted tapes.

For flows through packed fibrous beds the resistance for parallel fibers is about one-third that for perpendicular fibers

$$(Y_{\text{Ergun}} X_{\text{Ergun}})_{\text{parallel}} = 36k = \frac{1}{3} (Y_{\text{Ergun}} X_{\text{Ergun}})_{\text{perpendicular}} \quad (\text{A99})$$

These expressions agree with those presented by Hersh and Walker (1980), but an average of the two forms more closely approximates the data of Sullivan (1941)

$$X_{\text{Ergun}} Y_{\text{Ergun}} = \frac{46.6 + 58.8}{2} = 52.7 \quad (\text{A109})$$

and is similar to the reported (laminar) data (table 1 and eq. (A85)).

Single Twisted Tape

Parameters X_{Ergun} and Y_{Ergun} from the selected interpolated data of Date (1974), Koch (1958), Gambill and Bundy (1962), and Smithberg and Landis (1964) are plotted in figure 3 for the range $0.56 < H_o/D < \infty$. The dependency on H_o/D is evident and is bound by the porous-flow loci (eq. (A84)) to that of a single twisted tape at high Reynolds numbers (eq. (A83)). This conclusion is based on the data of Koch (1958), which were taken from figure 7 of Smithberg and Landis (1964).

The results of Sparrow and Haji-Sheikh (1966) for laminar flows can be expressed as (see page 17)

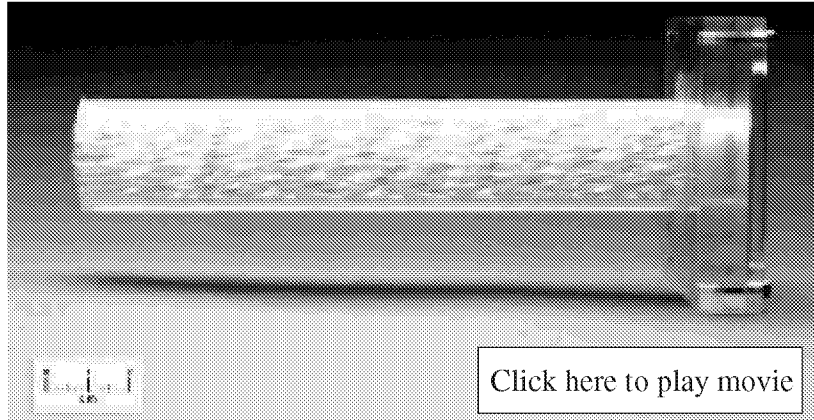
$$Y_{\text{Ergun}} X_{\text{Ergun}} = 70.94 \quad (\text{A39a})$$

Also plotted in figure 3 are the data for 48 twisted tapes in a tube along with equation (A84).

Figures 9 and 10 represent the loci of 48 twisted tapes in a tube, a single twisted tape in a tube, porous-media flows, and interpolated turbulent flow data for a single twisted tape in a tube corrected for swirl velocity.

VIDEOTAPE RECORDING

The complexity of the flow field, whether virtual or experimental, became vivid through the videotape recording, which is included as .avi and .mov files on the supplement CD in the printed version of this report. Visualization of the flow field reveals flow threads, wakes, stagnation zones, and the influence of the twisted-tape interfaces. The flow threads can be observed during a scan of the flow field from the front to rear lateral walls. These flow threads weave through the packed array of twisted tapes in the bulk flow direction. Details of the flow boundary layer close to the wall and progressing through the packed bed to the opposite wall are revealed. The video can also be used to determine quantitative experimental information, such as the flow velocities, by using the FFT technique (Braun et al., 1988).



SUMMARY OF RESULTS

The flow experiment consisted of three principal elements: an oil tunnel 7.6 cm by 7.6 cm (3 in. by 3 in.) in cross section, a cylindrical tube containing the packed bed of twisted tapes in an arbitrary array, and a flow characterization methodology, Full Flow Field Tracking (FFFT). The indices of refraction of the oil and the test matrix of twisted tapes were closely matched, and the flow was seeded with magnesium oxide particles. Planar laser light provided a two-dimensional projection of the flow field, and a traverse simulated a three-dimensional image of the entire flow field. Flows were observed near the inlet of the cylindrical tube housing the bundled array of twisted tapes, at the interface between the tube wall and the twisted tapes, and within the bundle of twisted tapes.

The flow field was three-dimensional and most complex to describe. The most prominent finding was flow threads. The axial flow appeared to spiral along the twisted tapes within the confines of a virtual distorted cylindrical boundary. The flow field appeared to be simulated by a packed array of very thin virtual cylinders, with the exception of the spiral effect due to the twist. The effects of random packing and bed voids created vortices and disrupted the laminar flow but minimized the entrance effects of the unpacked tube.

The results of several investigators for flows in geometries with a single twisted tape were analyzed. These results are related to the Ergun model in appendix A. (Symbols are defined in appendix B, and a comprehensive data table is given in table 1.) The single-twisted-tape results of Smithberg and Landis (1964) have been used to guide the analysis. The data for 48 twisted tapes in a tube were correlated by using the Ergun model for flows in porous media. The pressure drop and flow data for the three geometric configurations (Borda and orifice inlets with downstream restraining screen and orifice inlet without screen) have distinct flow characteristics differing up to 13%. The averages for the combined data sets were lower than the Ergun model by a factor of 3 for the packed bed of 48 twisted tapes in a tube and by a factor of nearly 1.6 for a single twisted tape in a tube. These results suggest a lower flow resistance for a packed bed of 48 twisted tapes in a tube than for either porous-media flows or single-twisted-tape flows. Further investigations including different geometric configurations and computational fluid dynamics analysis are suggested.

APPENDIX A

RESULTS OF SEVERAL INVESTIGATORS SCALED TO ERGUN MODEL

Because we really do not know how to correlate the data between a single twisted tape and multiple twisted tapes in a cylinder or tube (figs. 1 and 2), we will begin with some familiar definitions of friction factor and Reynolds numbers and arrive at the form similar to that developed by Ergun for porous-media flows.

$$\Delta P = \left(\frac{4f}{2} \right) \left(\frac{\rho u^2 L}{D_H} \right) \quad (\text{general Fanning friction factor}) \quad (\text{A1})$$

$$Re = \frac{\rho u D_H}{\mu}$$

and for now, let $\rho = \text{Constant}$ and $C_f = 4f$, as used, for example, by Sparrow and Haji-Sheikh (1966), Hong and Bergles (1976), and Gambill and Bundy (1962).

Now let us define some packed-bed parameters. Let the average or superficial velocity within a packed bed of one or more twisted tapes be

$$u = \frac{U}{\varepsilon} = \frac{U_o}{\varepsilon} \quad (\text{A2})$$

where U is the velocity in the tube without tapes. The bed porosity is defined as

$$\varepsilon = 1 - \frac{Ntw}{\pi \frac{D^2}{4}} \quad (\text{A3})$$

where N is the number of twisted tapes, t their thickness, w their width, and D_o the virtual twisted-tape diameter (fig. 2(c)).

$$D_o = \left(w^2 + t^2 \right)^{0.5} \quad (\text{A4})$$

We can now define the characteristic length of the packed bed in terms of sphere diameter. Note that $D_H = 4A/S$, where A is the cross section of the flow area and S the wetted perimeter. For a tube $D_H = D_{\text{tube}}$ and for a uniform bed of spheres $6V_s/A_s = 6/a_v = D_p \rightarrow D_{\text{sphere}}$ (Bird et al., 1960). This factor of 6:4 or 3:2 will become a scaling parameter for the Ergun relation. The characteristic length of the packed bed is

$$\frac{D_H}{4} = R_h = \frac{\varepsilon}{a} \quad (\text{A5})$$

where R_h is the ratio of the bed cross section available for flow to the wetted perimeter, which is equal to the ratio of the volume available for flow to the total wetted volume and is equal to the bed porosity divided by the ratio of the wetted surface to the bed volume. The specific surface area is

$$a_v = \frac{a}{1 - \varepsilon} = \frac{6}{D_p} \quad (\text{A6})$$

where α_v is equal to the ratio of the total sphere surface to its volume and is equal to the ratio of the wetted surface to the solid volume.

Combining equations (A5) and (A6) gives the characteristic length of the packed bed as

$$\frac{D_H}{4} = R_h = \frac{D_p \epsilon}{6(1-\epsilon)} \quad (\text{A7})$$

In terms of one or more of N twisted tapes contained within a cylinder or tube of diameter D , and with equation (A3),

$$D_H = \frac{4 \left(\frac{\pi D^2}{4} - Ntw \right)}{\pi D + 2N(t+w)} = \frac{D\epsilon}{1 + \frac{2N(t+w)}{\pi D}} \quad (\text{A8})$$

When equation (A8) is substituted into equation (A7), D_p becomes

$$D_p = \frac{\frac{3D}{2}(1-\epsilon)}{1 + \frac{2N(t+w)}{\pi D}} \quad (\text{A9})$$

Note that in figure 2(c) the dark shaded areas A, B, and C are within the bounds defined by the twisted-tape width w and thickness t , the tri-circular loci with radii of $D_o/2$, and the triangle with vertices 1,2,3. The area $B + \tilde{a} + \tilde{c} = wt/4$, the area $C - c + \tilde{b} = wt/4$, and the area $A - a - b = 0$. Therefore, the dark shaded area (solid area of the tape) within the triangle is $wt/2$. Continuing with triangle 4-2-1, $C_1 - c_1 + \tilde{b}_1 = wt/4$, $B_1 + \tilde{c}_1 + a = wt/4$, and $A_1 - \tilde{b}_1 - \tilde{a} = 0$. Similarly, for triangle 2-5-3, $C_2 - \tilde{c} + b_2 = wt/4$, $B_2 + c + \tilde{a}_2 = wt/4$, and $A_2 - b_2 - a_2 = 0$. Summing these areas gives the total solid twisted-tape area within the confines of the hexagon. Extending these results provides a generalized form for N twisted tapes within the confines of a hexagonal space that approximates that of a circumscribed cylinder or tube. This generalized form is an ideal model for packed beds that is expressed only in terms of tape width and thickness.

$$\epsilon_{\text{model}} = \frac{1 - 2 \frac{t}{2} \frac{w}{2}}{\frac{1}{2} D_o \frac{\sqrt{3}}{2} D_o} = 1 - \frac{2}{\sqrt{3}} \frac{tw}{t^2 + w^2} \quad (\text{A10})$$

and for $w = 2t$ (see also the section Some Sample Calculations at the end of this appendix)

$$\epsilon = 1 - \frac{4}{5\sqrt{3}} = 0.538$$

Comparing the model to the experiment where 48 twisted tapes with average width and thickness $\langle w \rangle = 0.3234$ cm (0.1273 in.) and $\langle t \rangle = 0.1275$ cm (0.0502 in.) were contained in a 2.54-cm- (1.0-in.-) diameter tube gives an average porosity, from equation (A3),

$$\langle \epsilon_{\text{exp}} \rangle = 1 - \frac{3}{2\pi} = 1 - \frac{192(0.3234)(0.1275)}{\pi(2.54)^2} = 0.61 \quad (\text{A11})$$

which indicates that the experimental test tube was well packed. For a single twisted tape in a tube (Smithberg and Landis, 1964), where $t = 0.0559$ cm (0.022 in.), $w \rightarrow D_o = 3.51$ cm (1.382 in.),

$$\varepsilon_{\text{Smithberg-Landis}} = 1 - \frac{4t}{\pi D_o} = 0.9797 \quad (\text{A12})$$

A problem arises because this formulation is independent of twist H/D . From structural mechanics the twisting of tapes is considered to follow linear mechanics with little change in length, unless plastic deformation with subsequent annealing takes place. As a result of this assumption the bed porosity is not a function of H . However, the flow path is a function of twist H/D , and consequently, the characteristic length must be modified to reflect H . The spiral path is defined in terms of the parameter φ as

$$x = r \cos \varphi; \quad y = r \sin \varphi; \quad Z = h\varphi \quad (\text{A12a})$$

and the path-length amplification ratio becomes, for the number of 2π twists n_t ,

$$\frac{L}{Z_o} = \frac{2\pi n_t r}{Z_o} \left[1 + \left(\frac{Z_o}{2\pi n_t r} \right)^2 \right]^{0.5} \quad (\text{A12b})$$

For very large H/D (slow spiral), $n_t \rightarrow 1$ and $L/Z_o \rightarrow 1$. For very small H/D (rapid spiral), $n_t \rightarrow M \gg 1$ and $L/Z_o \rightarrow 2\pi Mr/Z_o$. This amplification is not strong enough to account for the pressure drop increases due to the twist.

Models for Single-Twisted-Tape-in-Tube Analogy

Smithberg and Landis (1964).—Smithberg and Landis (1964) used the local average velocity (superficial bed velocity) in their correlations. Consequently, their friction factor and Reynolds number relations can be scaled directly in terms of the packed-bed parameters Y_{Ergun} and X_{Ergun} . Substituting equations (A2), (A7), and (A11) into equation (A1) gives the pressure drop parameter Y_{Ergun} in terms of the Darcy friction factor as

$$4f = 4f_{\text{Smithberg-Landis}} = \left(\frac{\Delta P}{0.5 \rho u^2} \right) \left(\frac{D_H}{L_o} \right) = \frac{1}{3} \left(\frac{\rho \Delta P}{G_o^2} \right) \left(\frac{\varepsilon^3}{1-\varepsilon} \right) \left(\frac{D_p}{L_o} \right) \quad (\text{A13})$$

$$f_{\text{Smithberg-Landis}} = \frac{1}{3} Y_{\text{Ergun}} \quad (\text{A14})$$

where

$$G_o = \rho U_o \quad (\text{A15})$$

$$Y_{\text{Ergun}} = \left(\frac{\rho \Delta P}{G_o^2} \right) \left(\frac{\varepsilon^3}{1-\varepsilon} \right) \left(\frac{D_p}{L_o} \right) \quad (\text{A16})$$

Here L_o represents the straight-line distance between pressure taps. The twisted-tape length L varies little from L_o over the practical range of tapes, and for laminar flows the correlated pressure drops are weakly dependent on twist H/D . However, for turbulent flows the pressure drop data are strongly twist dependent. In most cases $dp/dz \rightarrow \Delta P/L$ for single tapes in tubes. Therefore, in terms of Reynolds number the packed-bed Reynolds parameter X_{Ergun} becomes

$$\text{Re}_{\text{Smithberg-Landis}} = \frac{2\epsilon}{3} \left[\frac{G_o D_p}{(1-\epsilon)\mu} \right] = \frac{2\epsilon}{3} X_{\text{Ergun}} \quad (\text{A17})$$

where

$$X_{\text{Ergun}} = \frac{G_o D_p}{(1-\epsilon)\mu} \quad (\text{A18})$$

$$(f \text{Re})_{\text{Smithberg-Landis}} = \frac{2\epsilon}{9} Y_{\text{Ergun}} X_{\text{Ergun}} \quad (\text{A19})$$

For turbulent flows the $Y_{\text{Ergun}} X_{\text{Ergun}}$ product is dependent on both Re and H/D . Smithberg and Landis (1964) provide a simple expression for the Fanning friction factor. It is important to recall that herein we used $H/D = 180^\circ$ twist, whereas Smithberg and Landis used $H_o/D = 360^\circ$ twist, where H and H_o are measured along the axis parallel to the tube centerline.²

$$\frac{H_o}{D} = \left(\frac{H}{D} \right)_{\text{Smithberg-Landis}} = 2 \left(\frac{H}{D} \right) \quad (\text{A20})$$

$$f_{\text{Smithberg-Landis}} = \left[0.046 + 2.1 \left(\frac{H_o}{D} - 0.5 \right)^{-1.2} \right] \text{Re}^{-n} \quad (\text{A21})$$

where

$$n = 0.2 \left[1 + 1.7 \left(\frac{H_o}{D} \right)^{-0.5} \right]$$

Adjusting the constant 2.1 and the exponent -1.2 slightly gives a better fit to the data, and the normalized form becomes

$$\left[g_o \left(\frac{H_o}{D} \right) \right] = \left(\frac{f}{f_o} \right)_{\text{Smithberg-Landis}} = \left[1 + 105 \left(\frac{2H_o}{D} - 1 \right)^{-1.15} \right] \text{Re}_{\text{Smithberg-Landis}}^{-0.34/\sqrt{H_o/D}} \quad (\text{A22})$$

where $f_o = 0.046 \text{Re}^{-0.2}$. In terms of equation (A21), equation (A19) becomes

$$Y_{\text{Ergun}} X_{\text{Ergun}} = \frac{9}{2\epsilon} \left[g_o \left(\frac{H_o}{D} \right) \right] (f_o \text{Re})_{\text{Smithberg-Landis}} = \frac{0.207}{\epsilon} \left[g_o \left(\frac{H_o}{D} \right) \right] \text{Re}_{\text{Smithberg-Landis}}^{0.8} \quad (\text{A23})$$

After substituting equation (A17), equation (A23) becomes

$$Y_{\text{Ergun}} X_{\text{Ergun}} = 0.15 \epsilon^{0.8} \left[g \left(\frac{H}{D} \right) \right] X_{\text{Ergun}}^{0.8} \quad (\text{A24})$$

²Yet the number of 180° twists will be twice the number of 360° twists for a fixed tube length (i.e., $n_{180^\circ \text{ twists}} = 2n_{360^\circ \text{ twists}}$), and some authors use twist count rather than measured values of H and H_o .

where

$$\left[g\left(\frac{H}{D}\right) \right] = \left[1 + 105 \left(\frac{4H}{D} - 1 \right)^{-1.15} \right] \left(2\epsilon \frac{X_{\text{Ergun}}}{3} \right)^{-0.34/\sqrt{2H/D}}$$

At very high Reynolds numbers surface roughness will promote eddy bursts near the walls and separation effects as the flow attempts to track the twisted tape, implying that (figs. 8 and 10)

$$Y_{\text{Ergun}} \rightarrow \text{Constant} \rightarrow 0.014 \quad \text{for } \epsilon \rightarrow 1 \text{ and } \text{Re} \gg 2000 \quad (\text{A25})$$

where 0.014 is the commercial rough-tube equivalent (see eqs. (A54) and (A55)). For two-phase flows excessive vapor generation, or holdup, would be anticipated.

Hong and Bergles (1976).—A similar set of scaling parameters can be developed for the data of Hong and Bergles (1976):

$$\text{Re}_{\text{Hong-Bergles}} = \frac{\rho u D}{\mu} = \left(\frac{G_o D_p}{\mu} \right) \left(\frac{D}{D_p} \right) \left(\frac{D_p}{\epsilon} \right) \quad (\text{A26})$$

From equation (A8) with $N = 1$ and $(w + t) \rightarrow D$,

$$\frac{D}{D_p} = \frac{2}{3} \left(\frac{1 + 2 \frac{t+w}{\pi D}}{1 - \epsilon} \right) \rightarrow \frac{2}{3} \left(\frac{1 + \frac{2}{\pi}}{1 - \epsilon} \right) \rightarrow \frac{1.09}{1 - \epsilon} \quad (\text{A27})$$

$$\text{Re}_{\text{Hong-Bergles}} \rightarrow \frac{1.09}{\epsilon} X_{\text{Ergun}} \quad (\text{A28})$$

$$C_{f, \text{Hong-Bergles}} = \left(\frac{\Delta P}{0.5 \rho u^2} \right) \left(\frac{D}{L} \right) = 2 \left(\frac{\rho \Delta P}{G_o^2} \right) \left(\frac{D_p}{L} \right) \left(\frac{D}{D_p} \right) \epsilon^2 = 2 Y_{\text{Ergun}} \frac{2}{3} \left(\frac{1 + 2 \frac{t+w}{\pi d}}{\epsilon} \right) \rightarrow \frac{4}{3} \left(\frac{1 + \frac{2}{\pi}}{\epsilon} \right) Y_{\text{Ergun}} \quad (\text{A29})$$

where $L_o/L \rightarrow 1$. With $t = 0.046$ cm, $D_o = 1.02$ cm, and $w \rightarrow D_o$.

$$\epsilon_{\text{Hong-Bergles}} = 1 - \frac{0.046}{1.02 \frac{\pi}{4}} = 0.943 \quad (\text{A30})$$

Equation (A10) would give 0.945, so $w \rightarrow D_o$ is a good approximation.

$$C_{f, \text{Hong-Bergles}} = 2.314 Y_{\text{Ergun}} \quad (\text{A31})$$

For laminar flows in a half-tube configuration, equivalent to a tube with a single twisted tape,

$$(C_f \text{Re})_{\text{Hong-Bergles}} = \frac{8}{9} \left(\frac{1 + \frac{2}{\pi}}{\varepsilon} \right)^2 Y_{\text{Ergun}} X_{\text{Ergun}} = 183.6 \quad (\text{A32})$$

$$Y_{\text{Ergun}} X_{\text{Ergun}} = 68.6 \quad (\text{A33})$$

We will later show the relation to the work of Sparrow and Haji-Sheikh (1966) as

$$(C_f \text{Re})_{\text{Hong-Bergles}} = 183.6 = \left(\frac{D_H}{D} \right)^2 (C_f \text{Re})_{\text{Sparrow-Haji-Sheikh}} \quad (\text{A34})$$

where $D_H/D = 0.5682$ is found from equation (A8) by using the geometry of Hong and Bergles (1976), where $t = 0.046$ cm, $w = 0.97$ cm $\rightarrow D_o = 1.02$ cm, and $(D_H/D)^2 \rightarrow 0.334$.

Date (1974).—For the work of Date (1974) the scaling factors become, for $(t + w) \rightarrow D$,

$$\text{Re}_{\text{Date}} = \frac{\rho u d}{\mu} = \left(\frac{\rho U_o D_p}{\mu} \right) \left(\frac{D}{D_p} \right) = \frac{2}{3} \left(\frac{1 + \frac{2}{\pi}}{\varepsilon} \right) X_{\text{Ergun}} \quad (\text{A35})$$

$$f_{\text{Date}} = \frac{1}{2} \left(\frac{dp}{dz} \right) \left(\frac{D}{\rho u^2} \right) = \frac{1}{2} \left(\frac{dp}{dz} \right) \left(\frac{D_p}{\rho U_o^2} \right) \left(\frac{D}{D_p} \right) \varepsilon^2 = \frac{1}{3} \left(\frac{1 + \frac{2}{\pi}}{\varepsilon} \right) Y_{\text{Ergun}} \quad (\text{A36})$$

$$(f \text{Re})_{\text{Date}} = \frac{2}{9} \left(\frac{1 + \frac{2}{\pi}}{\varepsilon} \right)^2 Y_{\text{Ergun}} X_{\text{Ergun}} \quad (\text{A37})$$

For laminar flow in the half-tube configuration, or for a tube with a single twisted tape, and $\varepsilon \rightarrow 1$ (see Weigand, 1948, and eq. (A76))

$$f_{\text{Date}} \text{Re}_{\text{Date}} = 42.19 \quad (\text{A38})$$

$$Y_{\text{Ergun}} X_{\text{Ergun}} = 70.9 \quad (\text{A39})$$

which is in good agreement with equation (A33). For $\varepsilon = 0.934$, $Y_{\text{Ergun}} X_{\text{Ergun}} = 61.8$; and for $\varepsilon = 0.9797$, $Y_{\text{Ergun}} X_{\text{Ergun}} = 68.0$.

For $\text{Re}_{\text{Date}} < 150$, tape twist H/D has little influence on the Fanning friction factor. For $150 < \text{Re}_{\text{Date}} < 1000$,

$$f_{\text{Date}} = f_{\text{Date-half-tube}} + \Delta f_{\text{Date}}$$

$$\begin{aligned}
(f \text{Re})_{\text{Date}} &= f_{\text{Date-half-tube}} \text{Re}_{\text{Date}} \left(1 + \frac{\Delta f_{\text{Date}} \text{Re}_{\text{Date}}}{f_{\text{Date-half-tube}} \text{Re}_{\text{Date}}} \right) = 42.19 \left(1 + \frac{\Delta f_{\text{Date}} \text{Re}_{\text{Date}}}{42.19} \right) \\
&= \left[1 + \Delta f_{\text{Date}} \left(\frac{2}{3} \frac{1 + \frac{2}{\pi}}{\varepsilon} \right) \frac{X_{\text{Ergun}}}{42.19} \right] \frac{2}{9} \left(\frac{1 + \frac{2}{\pi}}{\varepsilon} \right)^2 Y_{\text{Ergun}} X_{\text{Ergun}}
\end{aligned} \tag{A40}$$

and for $\varepsilon \rightarrow 1$

$$Y_{\text{Ergun}} X_{\text{Ergun}} = 70.9 \left(1 + 0.026 \Delta f_{\text{Date}} X_{\text{Ergun}} \right) \tag{A41}$$

and for $150 < \text{Re}_{\text{Date}} < 1000$

$$\Delta f_{\text{Date}} = 0.088 \left[\left(\frac{D}{H} \right)_{\text{Date}} + 0.1 \left(\frac{D}{H} \right)_{\text{Date}}^{0.1} \right] \left[\log_{10} \frac{\text{Re}_{\text{Date}}}{150} \right] \tag{A41a}$$

For $\text{Re}_{\text{Date}} > 1000$, the Smithberg and Landis (1964) expression, or modified expression, for the Fanning friction factor can be converted to f_{Date} . Recall equation (A21):

$$f_{\text{Smithberg-Landis}} = \left[0.046 + 2.1 \left(\frac{H_o}{D} - 0.5 \right)^{-1.2} \right] \text{Re}^{-n} \tag{A21}$$

where

$$n = 0.2 \left[1 + 1.7 \left(\frac{H_o}{D} \right)^{-0.5} \right]$$

and the conversion for $\text{Re}_{\text{Date}} > 1000$ follows as

$$(f \text{Re})_{\text{Date}} = \left(\frac{D}{D_H} \right)^2 \left\{ 0.046 + 2.1 \left[\left(\frac{2H}{D} \right)_{\text{Date}} - 0.5 \right]^{-1.2} \right\} \text{Re}^{1-m} \tag{A42}$$

where

$$m = 0.2 \left\{ 1 + 1.7 \left[2 \left(\frac{H}{D} \right)_{\text{Date}} \right]^{-0.5} \right\}$$

The $D/D_H = 1.66$ given by Date (1974) should be nearly 1.6366. Date gives no values for tape width or thickness, and estimates of ε will give a range $61 < (Y_{\text{Ergun}} X_{\text{Ergun}})_{\text{Date}} < 71$ for laminar flow in a half-tube or in a tube with a single twisted tape. Also note that Date's calculations underpredict turbulent friction factor data by 30%.

Gambill and Bundy (1962) and Gambill et al. (1961) evaluate swirl-flow heat transfer along with isothermal data on friction coefficients. The relation given

$$(f_s - f_a)_{e\text{iso}} = \left(\frac{0.21}{y^{1.31}} \right) \left(\frac{\text{Re}_e}{2000} \right)^{-n} \quad (\text{A43})$$

where

$$n = 0.81 \exp \left[-1700 \left(\frac{\delta}{D_e} \right) \right] \quad (\text{A43a})$$

$$f_a = 4f_o = \left(\frac{-dp}{dx} \right) \left(\frac{D_e}{0.5\rho U^2} \right) \quad (\text{A43b})$$

$$D_e = \frac{4 \left(\frac{\pi D^2}{4} - tD \right)}{\pi D - 2t + 2D} \quad (\text{A43c})$$

and where y is the number of tube diameters per 180° of twist ($2n_tD$), D_e the equivalent or hydraulic diameter (over the practical range $5/4 < y < \infty$, $D_e \rightarrow D_H$), δ the surface roughness, f_s the Darcy swirl friction factor, and f_o the Fanning friction factor. The reduction of the analysis parameters to Ergun parameters takes the same form as that of Sparrow and Haji-Sheikh (1966):

$$f_a = C_f = \rho \left(\frac{-dp}{dz} \right) \frac{2}{3} \left(\frac{\varepsilon}{1-\varepsilon} \right) \frac{D_p}{0.5 \left(\frac{\rho U_o}{\varepsilon} \right)^2} = \frac{4}{3} Y_{\text{Ergun}} \quad \text{where } \frac{dp}{dz} \rightarrow \text{Constant} > 0 \quad (\text{A44})$$

$$\text{Re}_e = \left(\frac{\rho U_o}{\varepsilon} \right) \frac{2}{3} \left(\frac{\varepsilon}{1-\varepsilon} \right) \left(\frac{D_p}{\mu} \right) = \frac{2}{3} X_{\text{Ergun}} \quad (\text{A45})$$

However, the data presented in figure 2 of Gambill and Bundy (1962) follow the parameters of Hong and Bergles (1976):

$$\text{Re} = \text{Re}_{\text{Hong-Bergles}} \rightarrow \frac{1.09}{\varepsilon} X_{\text{Ergun}} \rightarrow 1.12 X_{\text{Ergun}} \quad (\text{A28a})$$

$$f_i = \left(\frac{\Delta P}{0.5 \rho u^2} \right) \left(\frac{D}{L} \right) = C_f, \text{ Hong-Bergles} \quad (\text{A29a})$$

$$f_i = C_{f, \text{Hong-Bergles}} = 2.314 Y_{\text{Ergun}} \quad (\text{A31a})$$

Equation (A43) represents the best fit of a large data set from several investigations, yet at $\text{Re}_e = 10\,000$ and $\delta/D = 6 \times 10^{-4}$ the ratio of friction factor data at $y = 1.12$ to those at $y = 0.28$ (an unusually tight twist) is nearly 17. From equation (A43) the ratio is 6. Although this difference has not been resolved, it is important to recognize that at a given Reynolds number and value of y (noting that $H/D = y/D$) the effect of surface roughness is very important because both increase the friction factor.

Sparrow and Haji-Sheikh (1966).—For the work of Sparrow and Haji-Sheikh (1966) on flow and heat transfer in an arbitrarily shaped tube, the scaling factors for the half-tube configuration become

$$C_f \text{Re} = \left(\frac{-dp}{dz} \right) \left(\frac{D_H}{0.5\rho u^2} \right) \left(\frac{\rho u D_H}{\mu} \right) = 63.06 \quad (\text{A46})$$

After substituting equations (A2) and (A7) and recalling our assertion that $dp/dz \rightarrow \Delta P/L$, equation (A1) becomes

$$C_f = \rho \left(\frac{-dp}{dz} \right) \frac{2}{3} \left(\frac{\epsilon}{1-\epsilon} \right) \left[\frac{D_p}{0.5 \left(\frac{\rho U_o}{\epsilon} \right)^2} \right] = \frac{4}{3} Y_{\text{Ergun}} \quad \text{where } \frac{-dp}{dz} \rightarrow \text{Constant} > 0 \quad (\text{A44a})$$

$$\text{Re} = \left(\frac{\rho U_o}{\epsilon} \right) \frac{2}{3} \left(\frac{\epsilon}{1-\epsilon} \right) \left(\frac{D_p}{\mu} \right) = \frac{2}{3} X_{\text{Ergun}} \quad (\text{A45a})$$

$$Y_{\text{Ergun}} X_{\text{Ergun}} = 70.94 \quad (\text{A39a})$$

Sparrow and Haji-Sheikh (1966) also estimate entrance losses as

$$C_f \left(\frac{z}{D_H} \right) + K = \frac{\Delta P}{0.5\rho u_{\text{bar}}^2} \quad (\text{A47})$$

where

$$K = \frac{2}{A} \int \left[\left(\frac{u}{u_{\text{bar}}} \right)^2 \left(1 - \frac{u}{u_{\text{bar}}} \right) \right] dA$$

and for the half-tube configuration

$$K \rightarrow 1.463 \quad (\text{A48})$$

The agreement between Sparrow and Haji-Sheikh (1966) and Date (1974) for the half-tube or single-twisted-tape configuration is not surprising as they are within 1% of the values of Weigand (1948), which we discuss in the section Torsion–laminar flow analogy.

Bird et al. (1960).—For laminar flow in a tube (limit $\epsilon \rightarrow 1$), Bird et al. (1960) give the average flow velocity as

$$u = \frac{\Delta P R_h^2}{2\mu L} \quad (\text{A49})$$

Substituting equations (A2) and (A7) and multiplying both sides by $\rho^2 U_o$ give

$$G_o^2 = 0.5 \left[\frac{\rho \Delta P \epsilon^3}{36(1-\epsilon)^2} \right] D_p^2 \left(\frac{G_o}{L_o} \right) \left(\frac{L_o}{L} \right) \quad (\text{A50})$$

$$1 = 0.5 \left(\frac{\frac{L}{L_o}}{\frac{36}{36}} \right) Y_{\text{Ergun}} X_{\text{Ergun}} \quad (\text{A51})$$

$$Y_{\text{Ergun}} X_{\text{Ergun}} = 72 \frac{L}{L_o} \quad \text{where } \frac{L}{L_o} \rightarrow 1 \quad (\text{A52})$$

which is in good agreement with the results of Date (1974), Sparrow and Haji-Sheikh (1966), Hong and Bergles (1976), and Weigand (1948) for laminar flows in the half-tube or single-twisted-tape configuration.

From data for flows in packed beds Bird et al. (1960) give $2L/L_o = 25/6$, resulting in the Blake-Kozeny equation. Kaviany (1995) gives $2L/L_o = 5$. From these results we anticipate that the bed correction factor for laminar flows in a configuration with N twisted tapes in a tube will be largely independent of the twist for

$$\text{Re}_{\text{Date}} = \frac{2}{3} \left(\frac{1 + \frac{2}{\pi}}{\varepsilon} \right) X_{\text{Ergun}} < 150 \quad \text{where } X_{\text{Ergun}} < 400 / 3 \text{ and } \varepsilon \rightarrow 1 \quad (\text{A53})$$

with some correction for flow path length $2L/L_o$. However, the correction factor will not be as strong as that for a randomly packed bed, where $X_{\text{Ergun}} < 10$ is considered laminar.

At high Reynolds numbers the results of Smithberg and Landis (1964) show significant effects of twist H_o/D as discussed earlier (eq. (A21)). At even higher Reynolds numbers the surface roughness will promote both eddy bursts near the walls and separation effects. For commercially rough tubes (Schlichting, 1955) and in the limit $\varepsilon \rightarrow 1$ (i.e., without a twisted tape in the tube)

$$(100\lambda \text{Re})_{\text{Nikuradse (1933)}} = 400 f \left(\frac{2\varepsilon}{3} \right) X_{\text{Ergun}} \approx \frac{400}{3} Y_{\text{Ergun}} \frac{2}{3} X_{\text{Ergun}} = 1.27 \quad (\text{A54})$$

$$Y_{\text{Ergun}} \rightarrow \text{Constant} \rightarrow 0.014 \quad \text{for } \varepsilon \rightarrow 1 \quad (\text{A55})$$

and 0.014 is the commercial rough-tube equivalent. From the data of Smithberg and Landis (1964) the trends for the single-twisted-tape or half-tube configuration, using D_H , appear to approach equation (A55).

Torsion-laminar flow analogy.—Weigand (1948) provides solutions to the problem of torsion in prismatic members where the function $f(x,y)$ satisfies (see also fig. 2(g))

$$\nabla^2 f = -1 \quad (\text{A56})$$

with $f_{\text{bar}} = 0$ on the boundary of the cross section. This function gives the torsion constant J_d for a member of cross section A , where

$$J_d = 4 \iint_A f dA \quad (\text{A57})$$

The analogy between fully developed flow in a tube and torsional problems starts with the Navier-Stokes equations

$$\frac{Du}{Dt} = F - \nabla p / \rho + \nu \nabla^2 u \quad (\text{A58})$$

assuming steady flow where inertia and body forces are small and $\nabla p = \text{Constant}$. It then follows that

$$\nabla^2 u = -1 \quad (\text{A59})$$

with $u_{\text{bar}} = 0$ on the boundary where

$$u_{\text{bar}} = \frac{\iint u dA}{A} \quad (\text{A60})$$

and

$$u = \frac{-dp}{dz} \frac{R^2}{4\mu} \left[1 - \left(\frac{r}{R} \right)^2 \right] = C_o \left[1 - \left(\frac{r}{R} \right)^2 \right] \quad (\text{A61})$$

The equations describing this type of flow are in a form similar to those for torsion in a prismatic bar as described by Weigand (1948) and pointed out by K.C. Cheng in a discussion to the work of Sparrow and Haji-Sheikh (1966). This leads to

$$\frac{R^2}{4C_o} \nabla^2 u = -1 = \nabla^2 f \quad (\text{A62})$$

$$f = \left(\frac{R^2}{4} C_o \right) u = u \left(\frac{-dp}{\frac{dz}{\mu}} \right)^{-1} \quad (\text{A63})$$

$$u_{\text{bar}} = \frac{\iint u dA}{A} = \iint f \left(\frac{-dp}{\frac{dz}{\mu}} \right) \frac{dA}{A} = \frac{J_d}{4} \left(\frac{-dp}{\frac{dz}{\mu}} \right) A^{-1} \quad (\text{A64})$$

Now the coefficient of friction and Reynolds number are related as

$$C_f \text{Re} = \left[\frac{\left(\frac{-dp}{dz} \right) D_e}{0.5 \rho u_{\text{bar}}^2} \right] \left(\frac{\rho u_{\text{bar}} D_e}{\mu} \right) = \frac{\left(\frac{-dp}{dz} \right) D_e^2}{0.5 u_{\text{bar}} \mu} \quad (\text{A65})$$

Substituting for u_{bar} for fully developed laminar flows, where $D_H = D_e$, gives

$$C_f \text{Re} = \frac{8AD_e^2}{J_d} \quad (\text{A66})$$

Substituting for

$$D_e = \frac{4A}{\text{Perimeter}} \quad (\text{A67})$$

gives

$$C_f \text{Re} = \frac{128A^3}{J_d(\text{Perimeter})^2} \quad (\text{A68})$$

where

$$A = \pi R^2 \left[1 - \left(\frac{2\alpha - \sin 2\alpha}{2\pi} \right) \right] \quad (\text{A69})$$

$$\text{Perimeter} = 2\pi R \left[1 - \frac{\alpha - \sin \alpha}{\pi} \right] \quad (\text{A70})$$

For circular tubes ($\chi = \pi - (\alpha = 0) \rightarrow \pi$) Weigand (1948) gives in his table IV

$$\kappa = \frac{J_d}{R^4} = 1.571 = \frac{\pi}{2} \quad (\text{A71})$$

and

$$C_f \text{Re} = 64 \quad (\text{A72})$$

For semicircular tubes [$\chi = \pi - (\alpha = \pi/2) \rightarrow \pi/2$] Weigand (1948) gives in his table IV

$$\kappa = \frac{J_d}{R^4} = 0.298 \quad (\text{A71a})$$

$$C_f \text{Re} = 16\pi \frac{\frac{R^4}{J_d}}{\left(1 + \frac{2}{\pi}\right)^2} = 62.97 \quad (\text{A73})$$

$$(C_f \text{Re})_{\text{Sparrow-Haji-Sheikh (1966)}} = 63.06 \quad (\text{A46a})$$

Although the $C_f \text{Re}$ values of Sparrow and Haji-Sheikh (1966) are monotone with α , those of Weigand (1948) are not. However, all are well represented by

$$C_f \text{Re} = 63 = \frac{128A^3}{J_d(\text{Perimeter})^2} \quad (\text{A74})$$

and would be a good engineering approximation for laminar flows in tubes of various cross sections (e.g., semicircular). For Date's work, using the preceding relations,

$$C_f \operatorname{Re} = 4f_i \left(\frac{D_e}{D} \right) \operatorname{Re}_i \left(\frac{D_e}{D} \right) = 4f_i \operatorname{Re}_i \left(\frac{D_e}{D} \right)^2 = 63 \quad (\text{A75})$$

and for the twisted tape under the following conditions:

$$\begin{aligned} y = \frac{H}{D} &\rightarrow \infty; & \alpha = \frac{\pi}{2}; & \frac{D}{D_e} = 1 + \frac{2}{\pi} \\ f_i \operatorname{Re}_i &= 42.19 \end{aligned} \quad (\text{A76})$$

Generalization.—For tubes with single twisted tapes

$$X_{\text{Ergun}} Y_{\text{Ergun}} = 70.9 + \left[g_1 \left(\frac{H}{D} \right) \right] \left(\frac{2\epsilon}{3} X_{\text{Ergun}} \right)^{1-n} \quad (\text{A77})$$

where from Smithberg and Landis (1964), for $X_{\text{Ergun}} > 2600/3$,

$$\left[g_1 \left(\frac{H}{D} \right) \right] = 0.046 + 2.1 \left(\frac{2H}{D} - 0.5 \right)^{-1.2} \quad (\text{A78})$$

and

$$n = 0.2 \left[1 + 1.7 \left(\frac{2H}{D} \right)^{-0.5} \right]$$

and for $400 < 3X_{\text{Ergun}} < 2600$

$$\left[g_1 \left(\frac{H}{D} \right) \right] = 0.088 \left[\frac{D}{H} + 0.1 \left(\frac{D}{H} \right)^{0.1} \right] \log_{10} \left[\left(\frac{2}{3} \frac{1 + \frac{2}{\pi}}{\epsilon} \right) \frac{X_{\text{Ergun}}}{150} \right] \quad (\text{A78a})$$

$$n = 1$$

Some consolidation in the turbulent flow regime follows from Smithberg and Landis (1964):

$$\frac{f}{f_{H/D \rightarrow \infty}} = 0.9 + \frac{6.9}{\frac{H_o}{D}} \quad (\text{A79})$$

where

$$f_{H/D \rightarrow \infty} = \frac{0.046}{\operatorname{Re}^{0.2}} \quad (\text{A79a})$$

and is thought of as the nonideal flow path length L for a particle to travel a bed or tube length of $(L_o)_{H/D \rightarrow \infty}$. Thus, $g_1(H/D)$ can be modified as

$$\left[g\left(\frac{H}{D}\right) \right] \approx 0.9 + \frac{6.9}{2H} \quad (A80)$$

Lopina and Bergles (1969).—Of equal interest is the simple relation given by Lopina and Bergles (1969) for turbulent flows in smooth tubes ($\pm 20\%$) for water and air for $5 \times 10^3 < Re < 4.5 \times 10^5$ and $\sqrt{3} < H/D < \sqrt{85}$:

$$\frac{f}{f_o} = 2.75 \left(\frac{H}{D} \right)^{-0.406} \quad (A81)$$

where f_o is the isothermal friction factor for an empty tube, $f_o = 0.046/Re^{0.2}$. Reducing the results of Lopina and Bergles (1969), with equation (A9), gives

$$f \text{Re} = \left(\frac{\Delta P D_i \rho}{2 L G^2} \right) \left(\frac{G D_i}{\mu} \right) \left(\frac{D_p}{D} \frac{\varepsilon}{\varepsilon} \frac{1-\varepsilon}{1-\varepsilon} \right)^2 \frac{\varepsilon}{\varepsilon} \quad (A81a)$$

$$f_o \text{Re} \left(\frac{f}{f_o} \right) = X_{\text{Ergun}} Y_{\text{Ergun}} 0.61 \left(\frac{H}{D} \right)^{-0.406} \frac{\left(1 + \frac{2}{\pi} \right)^2}{\varepsilon^3} \quad (A81b)$$

where

$$f = \left(\frac{1 + \frac{2}{\pi}}{3\varepsilon^3} \right) Y_{\text{Ergun}} \quad (A81c)$$

$$\text{Re} = \frac{2}{3} \left(1 + \frac{2}{\pi} \right) X_{\text{Ergun}} \quad (A81d)$$

The resulting fit to the data is lower than the data of Smithberg and Landis (1964) by about 10% for $H/D = 2.48$. So the agreement can be good and the simplicity may be of merit for a limited Reynolds number range.

We also note that for large values of X_{Ergun} the data will become independent of X_{Ergun} as equivalent surface roughness ($k_s \approx \delta/D$) plays a role. Thus, for large X_{Ergun} for a given geometry

$$Y_{\text{Ergun}} = \left[g_2 \left(\frac{H}{D}, k_s \right) \right] = \text{Constant} \quad (A82)$$

or in generalized terms

$$X_{\text{Ergun}} Y_{\text{Ergun}} = 70.9 + \left[g_2 \left(\frac{H}{D}, k_s \right) \right] X_{\text{Ergun}} \quad (A83)$$

and from extrapolating the data

$$X_{\text{Ergun}} Y_{\text{Ergun}} = 70.9 + 0.014 X_{\text{Ergun}} \quad (\text{A83a})$$

Porous Media Flows and N Twisted Tapes

For porous-media flows Ergun (1952) combined the turbulent and laminar data, noting that at high Reynolds numbers the friction factor approached a constant as is consistent with flow in a fully roughened tube ($k_s > 0$). The result was a linear sum of the Kozeny and Burke-Plummer equations, and as illustrated in Bird et al. (1960) the generalized form may be written

$$X_{\text{Ergun}} Y_{\text{Ergun}} = 150 + 1.75 X_{\text{Ergun}} \quad (\text{A84})$$

And if the Ergun data were for a single insert, and following the development on page 199 of Bird et al. (1960),

$$\rho^2 V_o^2 = \rho \Delta P \left(\frac{D_p}{L} \right) \left(\frac{\varepsilon^3}{1-\varepsilon} \right) \left(\frac{1}{72} \right) \left[\frac{\rho V_o D_p}{\mu (1-\varepsilon)} \right]$$

$$X_{\text{Ergun}} Y_{\text{Ergun}} = 72$$

which nearly coincides with the 70.9 of Lopina and Bergles (1969) in equation (A83), indicating that friction factors for flows in tubes with multiple twisted tapes should be much higher than measurements are showing.

For tubes with N twisted tapes the laminar data are below, yet parallel to, the $X_{\text{Ergun}} Y_{\text{Ergun}}$ relation for flows in porous media. From the data in table 1 (which may yet require Prandtl number or viscosity corrections),

$$X_{\text{Ergun}} Y_{\text{Ergun}} = \text{Constant} \doteq 45 \quad (\text{A85})$$

with a “suggested general form” for N twisted tapes in a tube following equation (A83), which appears as

$$X_{\text{Ergun}} Y_{\text{Ergun}} = 45 + 0.009 X_{\text{Ergun}} \quad (\text{A85a})$$

From equations (A93) and (A95) for parallel flows in cylindrical fibrous materials, with $\varepsilon = 0.61$ for a 48-twisted-tape cylindrical bundle,

$$X_{\text{Ergun}} Y_{\text{Ergun}} = 36k = 46.6 \quad (\text{A85b})$$

suggesting that pressure losses in the twisted-tape bundles are less than in other porous-media flows.

The combination of implied losses and those of, for example, cotton fibers, suggests a flow vortex structure that impedes the passage of fluids more than hair or glass fibers do. This structure does not suggest a direct relation to either heat or mass transfer. These implications remain to be investigated.

Fibrous Bulk Materials

The work of [Fowler and Hertel \(1940\)](#) for flows through wads (e.g., wool, glass wool, cotton, rayon, kapok) provides a solution:

$$G_o = \left(\frac{k \gamma_o}{2\mu} \right) \left(\frac{\tau}{\sigma} \right)^2 \left(\frac{\varepsilon^3}{(1-\varepsilon)^2} \right) \left(\frac{-dp^2}{dx} \right) \quad (\text{A86})$$

where $0.18 < k < 0.2$, $\gamma_o P = \rho$, and the specific surface area $a_v = \tau/\sigma$ equals the ratio of the element volume τ to the element surface σ . Equation (A86) can be rearranged to the Ergun form:

$$\frac{1}{X_{\text{Ergun}}} = \frac{(1-\varepsilon)\mu}{G_o D_p} = k \left(\frac{\tau}{\sigma} \right)^2 \left(\frac{\varepsilon^3}{1-\varepsilon} \right) \left(\frac{\rho}{G_o^2} \right) \left(\frac{-dp}{D_p} \right) = \left[\frac{k \left(\frac{\tau}{\sigma} \right)^2}{D_p^2} \right] Y_{\text{Ergun}} \quad (\text{A87})$$

where

$$Y_{\text{Ergun}} = \left(\frac{\rho \Delta P}{G_o^2} \right) \left(\frac{\varepsilon^3}{1-\varepsilon} \right) \left(\frac{D_p}{L_o} \right) \quad (\text{A16})$$

and

$$D_p = \frac{6}{a_v} = 6 \frac{\tau}{\sigma} \quad (\text{A88})$$

For $k = 0.2$

$$Y_{\text{Ergun}} X_{\text{Ergun}} = 180 \quad (\text{A89})$$

as also recommended by Kaviany (1995). For $k = 0.18$ as recommended by Fowler and Hertel (1940)

$$Y_{\text{Ergun}} X_{\text{Ergun}} = 200 \quad (\text{A90})$$

The work of Sullivan (1942) for parallel fibers illustrates a distinct departure from the relation $Y_{\text{Ergun}} X_{\text{Ergun}} = \text{Constant}$. Sullivan's relations are similar to those of Fowler and Hertel (1940) and follow the same reduction to the Ergun form:

$$D_p = \frac{6}{a_v} = \frac{6}{S_o} \quad (\text{A91})$$

$$\frac{1}{X_{\text{Ergun}}} = \frac{(1-\varepsilon)\mu}{G_o D_p} = \left(\frac{\zeta}{k_o S_o^2 D_p^2} \right) \left(\frac{\varepsilon^3}{1-\varepsilon} \right) \rho \Delta P \frac{D_p}{G_o^2} \quad (\text{A92})$$

$$Y_{\text{Ergun}} X_{\text{Ergun}} = 36k \quad (\text{A93})$$

where the units of Sullivan (1942) are in the cgs system (dyne, g, cm, s).

$$k = \frac{k_o}{\zeta} \quad (\text{A94})$$

and $\rho \equiv (\sin^2 \phi)_{\text{avg}}$, where ϕ is the angle between the interface normal and the microscopic flow. For flows with parallel "cylindrical" fibers and $\zeta \rightarrow 1$

$$k_{\zeta} \rightarrow k_o = \frac{\frac{\varepsilon}{3}}{1.02 - \varepsilon} + 0.8 \quad (\text{A95})$$

For flows with parallel cotton fibers and $\varepsilon < 0.85$

$$k_{\zeta} \rightarrow k_o = 2.5 \quad (\text{A96})$$

For $\varepsilon > 0.85$, $k_{\zeta} \rightarrow k_o$ tends to follow $k_{o,\text{parallel}}$.

The $Y_{\text{Ergun}} X_{\text{Ergun}}$ product for parallel flows in cotton fibers with $\varepsilon < 0.85$ is about half that cited by Fowler and Hertel (1940) for packed wads (90 versus 180 or 200 depending on the value of k used for packed wads of fibers) and would agree with Fowler and Hertel for packed-wad flows where $\varepsilon \rightarrow 0.95$. The k used by Sullivan is the inverse of that used by Fowler and Hertel.

[Hersh and Walker \(1980\)](#) revisited the work of Sullivan (1942) and provided a correlation over the range of data as follows, where the units are in the cgs system (dyne, g, cm, s):

For flow parallel to fibers ($0.1 < \varepsilon < 0.985$)

$$2f \text{Re} = \frac{\Delta P d^2}{\mu L U_o} = \left[\frac{15.74(1-\varepsilon)^{1.413}}{\varepsilon} \right] \left[1 + 27(1-\varepsilon)^3 \right] = F_{\text{parallel}}(\varepsilon) \quad (\text{A97a})$$

For flow perpendicular to fibers ($0.7 < \varepsilon < 0.992$)

$$2f \text{Re} = \frac{\Delta P d^2}{\mu L U_o} = 64 \left[\frac{(1-\varepsilon)^{3/2}}{\varepsilon} \right] \left[1 + 14.75(1-\varepsilon)^3 \right] = F_{\text{perpendicular}}(\varepsilon) \quad (\text{A97b})$$

where the latter expression was developed by Davies (1952).

After refitting the data of Sullivan (1942), the Hersh and Walker (1980) form may be re-expressed as

$$\left(\frac{\Delta P d^2}{\mu L U_o} \right)_{\text{parallel}} = \left(\frac{\frac{\varepsilon}{3}}{1.02 - \varepsilon} + 0.8 \right) \frac{16}{\varepsilon} \left(\frac{1-\varepsilon}{\varepsilon} \right)^2 = \frac{1}{3} \left(\frac{\Delta P d^2}{\mu L U_o} \right)_{\text{perpendicular}} \quad (\text{A98})$$

And the Ergun form follows:

$$(Y_{\text{Ergun}} X_{\text{Ergun}})_{\text{parallel}} = 36k = \frac{1}{3} (Y_{\text{Ergun}} X_{\text{Ergun}})_{\text{perpendicular}} \quad (\text{A99})$$

Although these expressions generally agree with those presented by Hersh and Walker (1980), an average of the two forms more closely approximates Sullivan's (1941) data (see figs. 2 and 3 in Hersh and Walker, 1980). These modified forms (eqs. (A97) and (A98)) are presented herein as figures 11 and 12.

Note that for parallel flows through cotton fibers the shape factor is 2.5, and for flows though fibers aligned normal to the flow (Davies, 1952) it is 3. The implication is that flows though fibrous materials (e.g., cotton) aligned with the flow do not differ significantly from flows through fibrous materials aligned normal to the flow. However, flows through fibrous materials still have three times the pressure drop as flows along parallel cylindrical materials when other parameters remain fixed. Sullivan (1941) found that the pressure drop through packed beds with fibers oriented perpendicular to the flow was double that of flows through parallel fibers.

Reducing the Hersh-Walker (1980) form to the Ergun (1952) form, noting that Sullivan gives $\langle d \rangle$ as follows from equations (A6) and (A7), results in

$$\frac{D_H}{4} = R_h = \frac{D_p \varepsilon}{6(1-\varepsilon)} = \left(\frac{1}{S_o} \right) \left(\frac{\varepsilon}{1-\varepsilon} \right) \quad (\text{A100})$$

where

$$\langle d \rangle = \frac{4}{S_o} = \frac{2D_p}{3} \quad (\text{A101})$$

Substituting, equation (A97) becomes

$$\left(\frac{\rho}{G_o^2} \right) \left(\frac{\varepsilon^3}{1-\varepsilon} \right) \Delta P \frac{\left(\frac{2D_p}{3} \right)^2}{L} = F(\varepsilon) \mu U_o \left(\frac{\rho}{G_o^2} \right) \left(\frac{\varepsilon^3}{1-\varepsilon} \right) \quad (\text{A102})$$

$$X_{\text{Ergun}} Y_{\text{Ergun}} = F(\varepsilon) \left(\frac{3}{2} \right)^2 \left(\frac{\varepsilon}{1-\varepsilon} \right)^2 \varepsilon \quad (\text{A103})$$

For flow parallel to the fibers ($0.1 < \varepsilon < 0.985$):

$$Y_{\text{Ergun}} X_{\text{Ergun}} = 35.415 \left[\left[(1-\varepsilon)^{-0.587} \varepsilon^2 \right] \left[1 + 27(1-\varepsilon)^3 \right] \right] \quad (\text{A104})$$

and, for reference, as $\varepsilon \rightarrow 0.27$ the quantity in braces approaches 1. Equation (A104) can be represented by $0.75 < \varepsilon < 1$.

$$(X_{\text{Ergun}} Y_{\text{Ergun}})^{1/4} = 1.6 - 0.7 \log_e(1-\varepsilon) \quad (\text{A104a})$$

For flow perpendicular to the fibers ($0.6 < \varepsilon < 0.992$):

$$Y_{\text{Ergun}} X_{\text{Ergun}} = 144 \left[\left[(1-\varepsilon)^{-0.5} \right] \varepsilon^2 \left[1 + 14.75(1-\varepsilon)^3 \right] \right] \quad (\text{A105})$$

Equation (A105) can be represented by $0.75 < \varepsilon < 1$.

$$(X_{\text{Ergun}} Y_{\text{Ergun}})^{1/4} = 2.5 - 0.8 \log_e(1-\varepsilon) \quad (\text{A105a})$$

and for this case the quantity in braces approaching 1 as $\varepsilon \rightarrow 0.5$ is beyond the region of validity of the relation.

From figures 11 and 12 (replotted figs. 2 and 3 from Hersh and Walker, 1980), the relations appear to be in good agreement, yet the sensitivity to small changes in ε becomes paramount. Compared with the twisted-tape data (see table 1) for $\varepsilon = 0.522$ and $N = 48$ twisted tapes in a cylindrical (parallel) bundle, equation (A104) gives $X_{\text{Ergun}} Y_{\text{Ergun}} = 58.8$, which is nearly $7/3$ greater than the data (see eq. (A85)). As the bed porosity approaches that of a filter or a particulate separator, the $X_{\text{Ergun}} Y_{\text{Ergun}}$ product is not a constant but depends on the filter porosity, as noted by Hersh and Walker (1980) and Sullivan (1942).

Silverman and First (1952) reported data for edge filtration of 0.5- μm dust and a baby-oil smoke generator with average 0.6- μm particulates. The filtration materials were a variety of felts, flocked papers, and fiberglass media. They noted that rockwool, silica fiber, or aluminum oxide fiber could be used at high temperatures. For their correlation

$$Y_{\text{Ergun}} X_{\text{Ergun}} = \frac{9}{4} 29 \varepsilon^3 (1 - \varepsilon)^{1.4} \quad (\text{A106})$$

Davies (1952) provides a theoretical foundation for several types of particulate separator, such as settling chambers, conical elutriators, inertial and cyclone separators, jet impingement mechanisms, precipitators, thermal separation mechanisms, and filters. Data for flow through fibrous materials follow:

$$Y_{\text{Ergun}} X_{\text{Ergun}} = \frac{9}{4} (70) \varepsilon (1 - \varepsilon)^{1.5} [1 + 52(1 - \varepsilon)^{1.5}] \quad (\text{A107})$$

The Davies (1952) results range up to three times higher than those of Silverman and First (1952) to several times higher than those of Hersh and Walker (1980).

Using the data in table 1 for 48 twisted tapes in a cylindrical (parallel) bundle, where $\varepsilon = 0.522$, gives,

$$X_{\text{Ergun}} Y_{\text{Ergun}} = 58.8 \quad \text{from eq. (A104)} \quad (\text{A108a})$$

$$X_{\text{Ergun}} Y_{\text{Ergun}} = 46.6 \quad \text{from eq. (A85b)} \quad (\text{A108b})$$

For the 48-twisted-tape data prediction

$$X_{\text{Ergun}} Y_{\text{Ergun}} = \frac{46.6 + 58.8}{2} = 52.7 \quad (\text{A109})$$

or less than 1.2 times that of the reported data (table 1 and eqs. (A85)).

Packed Beds of Spheres

Wentz and Thodos (1963) measured the pressure drop across packed (cubic, body centered, and face centered) and distended bands of five layers of 3.12-cm- (1.23-in.-) diameter spheres held in place by short wires in drilled holes and epoxy. Spheres in the distended models were separated to simulate bed swelling. Both sets of data were correlated by

$$Y_{\text{Ergun}} = \frac{0.396}{X_{\text{Ergun}}^{0.05} - 1.2} \quad 2550 < X_{\text{Ergun}} < 64\,900 \quad (\text{A110})$$

which is less than half that of the Ergun equation (A84) but over a larger range of X_{Ergun} . As the bed length was short (five spheres), X_{Ergun} dependence may be attributed to as-yet-undeveloped turbulent flow. A problem combining or extending this relation occurs with the laminar regime because a singularity occurs at $X_{\text{Ergun}} = 38.34$. However,

$$X_{\text{Ergun}} Y_{\text{Ergun}} = 150 + 4.5 X_{\text{Ergun}}^{0.84} \quad (\text{A111})$$

is a form that includes this high- X_{Ergun} turbulent regime, yet is higher than the Ergun equation (A84) for the transition region $15 < X_{\text{Ergun}} < 300$ and as much as 14% higher for the region $40 < X_{\text{Ergun}} < 80$ (fig. 13). The

turbulent-flow pressure drops through these packed beds of spheres have similar X_{Ergun} dependence yet are 30 to 40 times larger than for a single twisted tape in a tube over similar ranges in X_{Ergun} . The expression

$$X_{\text{Ergun}} Y_{\text{Ergun}} = 0.03 [150 + 4.5 X_{\text{Ergun}}^{0.84}] \quad (\text{A112})$$

provides a reasonable fit to the data of Smithberg and Landis (1964) and Koch (1958) in figure 14.

Some Sample Calculations

The basic parameters for 48 twisted tapes in a 2.54-cm- (1.0-in.-) diameter tube are as follows:

Fluid:

$$\rho = 0.9 \text{ g/cm}^3$$

$$\mu = 0.9 \text{ g/cm-s}$$

Tapes: $\langle w \rangle$ and $\langle t \rangle$ represent average values of twisted-tape width and twisted-tape thickness measured at each end of the 48 twisted tapes (table 2).

$$\langle w \rangle = w = 0.3234 \text{ cm (0.1273 in.)}$$

$$\langle t \rangle = t = 0.1275 \text{ cm (0.0502 in.)}$$

$$D_o = (w^2 + t^2)^{0.5} = 0.348 \text{ cm (0.137 in.)}$$

Three full 360° twists in 16.5-cm (6.5-in). length provides an average twist ratio of

$$\frac{H_o}{D_o} = \frac{\frac{16.5}{3}}{0.348} = 15.8$$

$$\frac{H}{D_o} = 7.9$$

$$L_o = 16.5 \text{ cm}$$

Other parameters: $\langle \epsilon_{\text{exp}} \rangle = 0.61$ is the average area-weighted porosity ($0.593 < \epsilon_{\text{exp}} < 0.628$).

$$\epsilon_{\text{exp}} = 0.61$$

$$D_p = \frac{\frac{3}{2} D(1-\epsilon)}{1 + \frac{2N(t+w)}{\pi D}} = \frac{(1.5)(2.54)(0.39)}{1 + (2)(48)\left(\frac{0.1275 + 0.3234}{(2.54)\pi}\right)} = 0.231 \text{ cm}$$

$$A_o = 2.54^2 \left(\frac{\pi}{4}\right) = 5.067 \text{ cm}^2$$

$$G_o = \frac{\rho \frac{dV}{dt}}{A_o} = \frac{\frac{dV}{dt} \frac{0.9}{60}}{5.067} = 2.96 \times 10^{-3} \dot{V} \quad \text{where } \dot{V} \text{ is in cm}^3 / \text{min}$$

$$\Delta P = dP \left(6.8947 \times 10^4 \right) \quad \text{in g/cm-s}^2, \text{ where } P \text{ is in psia}$$

$$X_{\text{Ergun}} = \frac{G_o D_p}{(1-\varepsilon)\mu} = G_o \left[\frac{0.231}{(0.39)(0.9)} \right] = 0.659 G_o \quad \text{where } G_o \text{ is in g/cm}^2 \cdot \text{s}$$

$$Y_{\text{Ergun}} = \left(\frac{\rho \Delta P}{G_o^2} \right) \left(\frac{D_p}{L_o} \right) \left(\frac{\varepsilon^3}{1-\varepsilon} \right) = \frac{(0.9)(0.61)^3}{0.39} \frac{0.231}{16.5} \frac{\Delta P}{G_o^2} = 73.34 \times 10^{-4} \frac{dP}{G_o^2}$$

$$Y_{\text{calc}} = \frac{150}{X_{\text{Ergun}}} + 1.75$$

Data

Date	Geometry	dV/dt , cm ³ /min	ΔP , psi	G_o , g/cm ² -s	dP , g/cm-s ²	X_{Ergun}	Y_{Ergun}	Y_{calc}	$Y_{\text{calc}}/Y_{\text{Ergun}}$
12-10-98	Borda + screen	5900	2.54	17.46	17.5×10^4	11.5	4.22	14.8	3.51
12-14-98	Orifice + screen	4754	1.88	14.07	13.0×10^4	9.27	4.81	17.9	3.73
12-14-98	Orifice - screen	6767	2.47	20.0	17.0×10^4	13.2	3.12	13.1	4.21
12-14-98	Borda + screen	6777	2.86	20.0	19.7×10^4	13.22	3.6	13.1	3.64
12-19-98	Orifice + screen	6556	2.48	19.4	17.1×10^4	12.79	3.33	13.5	4.04

For all the data (see table 1)

$$\frac{Y_{\text{calc}}}{Y_{\text{Ergun}}} = 3.6^{+0.7}_{-0.6} \quad \text{Standard deviation, 0.32}$$

$$Y_{\text{Ergun}} X_{\text{Ergun}} = 45^{+6}_{-5} \quad \text{Standard deviation, 3.5}$$

For the minimum and maximum twisted-tape thickness and width, from table 2, and the combined data set of table 1,

$\langle t \rangle$	$\langle w \rangle$	$\langle \varepsilon_{\text{exp}} \rangle$	$Y_{\text{cal}}/Y_{\text{Ergun}}$	Standard deviation
0.1235 cm (0.0486 in.)	0.318 cm (0.1252 in.)	0.6276	3.2	0.28
0.1296 cm (0.051 in.)	0.3287 cm (0.1294 in.)	0.5934	4	0.35

where $\langle \varepsilon_{\text{exp}} \rangle$ is the area-averaged porosity and

$$39 < Y_{\text{Ergun}} X_{\text{Ergun}} < 51$$

However, the data sets for the Borda and orifice with screen and the orifice without screen have distinct flow characteristics, and more representative values of $Y_{\text{Ergun}} X_{\text{Ergun}}$ can be determined. For the 48-twisted-tape data of table 1, the coefficients of the least-squares trend line

$$\log_{10}[Y_{\text{Ergun}}] = A_1 \log_{10}[X_{\text{Ergun}}] + B_1$$

through individual data sets are tabulated below, where R^2 is the regression coefficient.

Flow configuration	A_1	B_1	R^2	Constant $\approx Y_{\text{Ergun}} X_{\text{Ergun}}$
Average porosity = 0.61				
Borda with screen ^a	-0.9873	1.6673	0.9965	46.5
Orifice with screen	-1.0006	1.6436	.9984	44.0
Orifice without screen	-0.9982	1.6132	.9988	41.0
Combined data sets	-0.9867	1.6469	.992	44.4
Minimum porosity = 0.5934				
Borda with screen ^a	-0.9879	1.6202	0.9964	41.7
Orifice with screen	-1.0006	1.5958	.9984	39.4
Orifice without screen	-0.9982	1.5655	.9988	36.8
Combined data sets	-0.9869	1.5994	.992	39.8
Maximum porosity = 0.6276				
Borda with screen ^a	-0.9866	1.7190	0.9966	52.4
Orifice with screen	-1.0006	1.6961	.9984	49.7
Orifice without screen	-0.9982	1.6658	.9988	46.3
Combined data sets	-0.9864	1.699	.9919	50.0

^aOne questionable data point set at average of previous and following points in table 1.

Estimates from figure 6 of Smithberg and Landis (1964) for air and water data are

$$X_{\text{Ergun}} = \frac{3 \text{Re}}{2}$$

$$Y_{\text{Ergun}} = 3f$$

	Reynolds number, Re				
	5000	10 000	20 000	40 000	60 000
	X_{Ergun}				
	7500	15 000	30 000	60 000	90 000
f at $H_o/D = 3.62$	29×10^{-3}	21×10^{-3}	15.5×10^{-3}	13×10^{-3}	12.5×10^{-3}
Y_{Ergun}	87×10^{-3}	63×10^{-3}	46.5×10^{-3}	39×10^{-3}	37.5×10^{-3}
f at $H_o/D = 4.34$	22.5×10^{-3}	16.5×10^{-3}	13×10^{-3}	11×10^{-3}	9.7×10^{-3}
Y_{Ergun}	67.5×10^{-3}	49.5×10^{-3}	39×10^{-3}	33×10^{-3}	29.1×10^{-3}
f at $H_o/D = 10.3$	14×10^{-3}	11×10^{-3}	8.5×10^{-3}	7.4×10^{-3}	6.8×10^{-3}
Y_{Ergun}	42×10^{-3}	33×10^{-3}	25.5×10^{-3}	22.2×10^{-3}	20.4×10^{-3}
f at $H_o/D = 22$	12×10^{-3}	9.9×10^{-3}	7.6×10^{-3}	6.6×10^{-3}	6×10^{-3}
Y_{Ergun}	36×10^{-3}	29.7×10^{-3}	22.8×10^{-3}	19.8×10^{-3}	18×10^{-3}
f at $H_o/D = \infty$	8×10^{-3}	7.1×10^{-3}	6×10^{-3}	5.35×10^{-3}	5×10^{-3}
Y_{Ergun}	24×10^{-3}	21.3×10^{-3}	18×10^{-3}	16.1×10^{-3}	15×10^{-3}

The Smithberg and Landis (1964) data ($N = 1$) are Reynolds number dependent. It would be interesting to determine if data for $N = 2, 3, \dots, 48$ form parametric families that become more independent of Reynolds number as N increases (see eq. (A55)).

Estimates from Koch (1958) as provided from figure 7 of Smithberg and Landis (1964) are as follows:

	Reynolds number, Re						
	2000	3000	6000	10 000	20 000	30 000	50 000
	X_{Ergun}						
	3000	4500	9000	15 000	30 000	45 000	75 000
f at $H/D = 5$	32.5×10^{-3}	26.5×10^{-3}	18×10^{-3}	14.6×10^{-3}	11.6×10^{-3}	10×10^{-3}	9×10^{-3}
Y_{Ergun}	97.5×10^{-3}	79.5×10^{-3}	54×10^{-3}	43.8×10^{-3}	34.8×10^{-3}	30×10^{-3}	27×10^{-3}
f at $H/D = 8.5$	21×10^{-3}	17.5×10^{-3}	13.2×10^{-3}	10.9×10^{-3}	8.6×10^{-3}	7.5×10^{-3}	6.4×10^{-3}
Y_{Ergun}	63×10^{-3}	52.5×10^{-3}	39.6×10^{-3}	32.7×10^{-3}	25.8×10^{-3}	22.5×10^{-3}	19.2×10^{-3}
f at $H/D = 22$	14.2×10^{-3}	12.3×10^{-3}	9.7×10^{-3}	8.5×10^{-3}	7.1×10^{-3}	6.4×10^{-3}	5.7×10^{-3}
Y_{Ergun}	42.6×10^{-3}	36.9×10^{-3}	29.1×10^{-3}	25.5×10^{-3}	21.3×10^{-3}	19.2×10^{-3}	17.1×10^{-3}
f at $H/D = \infty$	10×10^{-3}	9.5×10^{-3}	8.1×10^{-3}	7.4×10^{-3}	6.5×10^{-3}	5.9×10^{-3}	5.4×10^{-3}
Y_{Ergun}	30×10^{-3}	28.5×10^{-3}	24.3×10^{-3}	22.2×10^{-3}	19.5×10^{-3}	17.7×10^{-3}	16.2×10^{-3}

SUMMARY TABLE

Researcher	Flow configuration	Type of flow	Form of Ergun relation ^a	Text equation
Smithberg-Landis (1964)	Tube with single twisted tape	Turbulent	$Y_{\text{Ergun}} X_{\text{Ergun}} = 0.15 \varepsilon^{0.8} 0 \left[g \left(\frac{H}{D} \right) \right] X_{\text{Ergun}}^{0.8}$	(A24) and following, (A25)
Hong-Bergles (1976)	Tube with single twisted tape	Laminar	$\left(C_f \text{Re} \right)_{\text{Hong-Bergles}} = \frac{8}{9} \left(1 + \frac{2}{\varepsilon} \right)^2 Y_{\text{Ergun}} X_{\text{Ergun}} = 183.6$	(A32), (A33)
Date (1974)	Single tube with twisted tape	Laminar (and turbulent ^b)	$Y_{\text{Ergun}} X_{\text{Ergun}} = 68.6$	(A39)
Sparrow-Hajji-Sheikh (1966)	Single tube with arbitrary geometry	Laminar and numerical	$Y_{\text{Ergun}} X_{\text{Ergun}} = 70.94$	(A39a), (A46)
Bird et al. (1960)	Packed beds, porous media	Laminar	$C_f \text{Re} = \left(\frac{-dp}{dz} \right) \left(\frac{D_H}{0.5 \mu u^2} \right) \left(\frac{\rho u D_H}{\mu} \right) = 63.06$	
Weigand (1948)	Torsion in prismatic rods	Torsion-laminar flow analogy	$Y_{\text{Ergun}} X_{\text{Ergun}} = 72 \frac{L}{L_o}$ where $\frac{L}{L_o} \rightarrow 1$	(A52)
Generalization of flows in “tubes”	Twisted tapes with roughness	Laminar and turbulent	$C_f \text{Re} = 63 = \frac{128 A^3}{J_d (\text{Perimeter})^2}$ $Y_{\text{Ergun}} X_{\text{Ergun}} = 70.9$	(A74), (A39)
Lopina-Bergles (1969)	Twisted tapes with $f \text{Re} / f_c$ normalized	Turbulent	$X_{\text{Ergun}} Y_{\text{Ergun}} = 70.9 + \left[g_2 \left(\frac{H}{D}, k_s \right) \right] X_{\text{Ergun}}$	(A83)
Hendricks et al. (1997)	48-twisted-tape cylindrical pack	Laminar	$f_o \text{Re} \left(\frac{f}{f_o} \right) = X_{\text{Ergun}} Y_{\text{Ergun}} 0.61 \left(\frac{H}{D} \right)^{-0.406} \frac{\left(1 + \frac{2}{\pi} \right)^2}{\varepsilon^3}$ $X_{\text{Ergun}} Y_{\text{Ergun}} = 45 + 0.009 X_{\text{Ergun}}$	(A81b) (A85a) ^c

Fowler-Hertel (1940)	Fibrous materials and packed wads	Unstated	$Y_{\text{Ergun}} X_{\text{Ergun}} = 200$	(A90)
Sullivan (1942)	Fibrous materials	Unstated	$Y_{\text{Ergun}} X_{\text{Ergun}} = 36k$	(A93), (A94), (A95), (A96)
			$k = \frac{k_o}{\zeta}$	
			$k\zeta \rightarrow k_o = \frac{\epsilon}{1.02 - \epsilon} + 0.8$	for parallel fibers
			$k\zeta \rightarrow k_o = 2.5$	for parallel cotton fibers
Hersh-Walker (1980), Sullivan (1942), Davies (1952)	Fibrous materials ^d	Unstated	$\left(Y_{\text{Ergun}} X_{\text{Ergun}} \right)_{\text{parallel}} = 36k = \frac{1}{3} \left[Y_{\text{Ergun}} X_{\text{Ergun}} \right]_{\text{perpendicular}}$	(A99)
Hersh-Walker (1980), Sullivan (1942)	Fibrous materials ^d with flow parallel to fibers	Unstated	$Y_{\text{Ergun}} X_{\text{Ergun}} = 35.415 \left[(1-\epsilon)^{-0.587} \epsilon^2 \right] \left[1 + 27(1-\epsilon)^3 \right]$	(A104)
Hersh-Walker (1980), Sullivan (1942)	Fibrous materials ^d with flow perpendicular to fibers	Unstated	$Y_{\text{Ergun}} X_{\text{Ergun}} = 144 \left[(1-\epsilon)^{-0.5} \epsilon^2 \right] \left[1 + 14.75(1-\epsilon)^3 \right]$	(A105)
Silverman and First (1962)	Filtration materials	Unstated	$Y_{\text{Ergun}} X_{\text{Ergun}} = \frac{9}{4} 29\epsilon^3 (1-\epsilon)^{1.4}$	(A106)
Davies (1952)	Fibrous filter materials	Unstated	$Y_{\text{Ergun}} X_{\text{Ergun}} = \frac{9}{4} (70)\epsilon(1-\epsilon)^{1.5} \left[1 + 52(1-\epsilon)^{1.5} \right]$	(A107)
Gambill-Bundy (1962)	Twisted tape and swirlers	Laminar and turbulent	$(f_s - f_a)_{e_{\text{iso}}} = \left(\frac{0.21}{y^{1.31}} \right) \left(\frac{\text{Re}_e}{2000} \right)^{-n}$ $n = 0.81 \exp \left[-1700 \left(\frac{\delta}{D_e} \right) \right]$ $f_a = 4f_o = \left(\frac{-dp}{dx} \right) \left(\frac{D_e}{0.5\rho U^2} \right)$	(A43), (A43a), (A43b)

^aIt is important to note that $f/\text{Re} = \text{(function)} = (\text{conversion}) X_{\text{Ergun}} Y_{\text{Ergun}}$, and $C_f = 4f_o$.

^bTurbulent calculations were approximately 30% lower than the data; equation not shown.

^cSuggested general form is eq. (A85a).

^dReanalysis.

APPENDIX B

SYMBOLS

A	flow area
A_1	constant
A_o	tube cross-sectional area without twisted tape
A_s	surface area or area of sphere
a	ratio of wetted surface area to bed volume
a_v	specific surface area, τ/σ
B_1	constant
C_f	flow coefficient of friction
C_o	constant relating velocity profiles to radial position
D	tape diameter or width (for thin tubes, same as flow tube diameter)
D_e	equivalent diameter
D_H	hydraulic diameter; characteristic length of packed bed
D_i	inside diameter
D_o	virtual diameter of twisted tape
D_p	equivalent particle diameter
D_{sphere}	sphere diameter
D_{tube}	flow tube diameter
d	fiber diameter
$\langle d \rangle$	average fiber diameter
e_{iso}	subscript denoting equivalent isothermal, eq. (A43)
$F(\epsilon)$	function relating friction to flow direction, eqs. (A97)
f	Fanning friction factor, $\left(\frac{D}{4L} \right) \left(\frac{dp/dx}{0.5\rho u^2} \right)$
f_a	no-swirl friction factor, eq. (A43b)
f_i	friction factor, eq. (A75)
f_o	Fanning friction factor for tube without twisted tape
f_s	Darcy swirl (twisted tape) friction factor, $f_s = 4f$ (Darcy $f = 4$ Fanning f)
G	mass flow, ρu
G_o	mass flux, $\rho U_o = W/A_o$
g	function defined in eq. (A24)
g_o	function defined in eq. (A23)
g_1	function defined in eqs. (A78)
g_2	function defined in eq. (A82)
H	tape twist through 180° or one-half full wave
H_o	tape twist through 360° or one full wave
J_d	torsion constant
K	entrance pressure loss parameter, eq. (A47)
k	packing constant, k_o/ζ , eqs. (A86) and (A94)
k_o	porosity shape parameter, eq. (A94)

k_s	surface roughness parameter
L	equivalent flow or twisted-tape length; nonideal flow path length
L_o	tape length without twist; straight-line distance between pressure taps; bed or tube length
M	number much greater than unity
m	exponent, eq. (A42)
m_1	number much less than unity
N	number of twisted tapes in tube
n	exponent, eqs. (A21) and (A43)
n_t	number of 2π twists
P	pressure, experimental
p	pressure, calculated
R	outer radius
R_h	ratio of bed cross section available for flow to wetted perimeter
Re	Reynolds number, $\rho u D / \mu$
Re_e	equivalent Reynolds number
Re_i	Reynolds number, eq. (A75)
r	radial position
r_o	outer “wall” radius
S	wetted perimeter; surface area of fibrous specimen
S_o	surface area, eq. (A101)
t	tape thickness
$\langle t \rangle$	average twisted-tape thickness
U	bulk average axial velocity
U_e	equivalent fluid velocity
U_o	empty or unpacked-bed velocity
u	velocity, general or vector; superficial velocity
\bar{u}_{bar}	average velocity
V	bed volume
\dot{V}	volumetric flow rate
V_s	volume of sphere
V_{solid}	volume of solid in porous bed
V_{total}	total bed volume (solid plus void)
v	flow velocity in fibrous specimen
v_θ	circumferential velocity; tangential fluid velocity
v_o	velocity at r_o
v_t	tangential velocity
W	mass flow rate
w	twisted-tape width
$\langle w \rangle$	average twisted-tape width
X_{Ergun}	Ergun Reynolds number parameter, $G_o D_p / (1 - \varepsilon) \mu$
X_n	pressure drop data parameter
x	axial position
Y_{calc}	calculated Ergun parameter

Y_{Ergun}	Ergun friction factor parameter, $(\rho \Delta P / G_o^2) [\varepsilon^3 / (1 - \varepsilon)] [D_p / L_o]$
Y_n	flow data parameter
y	number of tube diameters per 180° of twist (also used as coordinate, fig. 2(e))
Z	analytical axial locus
Z_o	equivalent axial distance without twist
z	axial coordinate
α, ϕ, χ	polar coordinate parameters, fig. 2(e)
δ	surface roughness
γ_o	bulk density parameter, eq. (A86)
ε	bed porosity parameter
ε_{exp}	experimental bed porosity
$\varepsilon_{\text{model}}$	modeled bed porosity
κ	torsion parameter, eq. (A71)
ρ	average fluid density
μ	viscosity
v	$\frac{\mu}{\rho}$ kinematic velocity
φ	analytical twist parameter
ϕ	angle between interface normal and microscopic flow
τ/σ	surface-to-volume parameter, eq. (A86)
τ	thickness of fibrous specimen
σ	deviation
ζ	porosity parameter, eq. (A94)

REFERENCES

- Bergles, A.E. (1998) Augmentation of Heat Transfer, 2.5.11 in Heat Exchanger Design Handbook 1998, G.F. Hewitt, ex. ed., Part 2 Fluid Mechanics and Heat Transfer, Begell House, Inc., New York.
- Bird, R.B., Stewart, W.E., and Lightfoot, E.N. (1960) Transport Phenomena, John Wiley & Son, New York.
- Braun, M.J., Batur, C., and Karavelakis, G. (1988) Digital Image Processing for Quantification Through Full Flow Field Tracking (FFFT) in Narrow Geometries at Low Reynolds Numbers, AIAA Paper 88-3781.
- Date, A.W. (1974) Prediction of Fully Developed Flow in a Tube Containing a Twisted Tape, *Int. J. Heat and Mass Trans.*, vol. 17, pp. 845-859.
- Davies, C.N. (1952) The Separation of Airbourne Dust and Particles, *Proc. Inst. Mech. Engrs. (London)*, B1, pp. 185-198.
- Ergun, S. (1952) Fluid Flow Through Packed Columns, *Chem. Eng. Prog.*, vol. 48, no. 2, pp. 89-93.
- Fowler, J.L. and Hertel, K.L. (1940) Flow of a Gas Through Porous Media, *J. Appl. Phys.*, vol. 11, pp. 496-502.
- Gambill, W.R. and Bundy, R.D. (1963) High-Flux Heat Transfer Characteristics of Pure Ethylene Glycol in Axial and Swirl Flow, *A.I.Ch.E. Journal*, vol. 9, no. 1, p. 55.
- Gambill, W.R. and Bundy, R.D. (1962) An Evaluation of the Present Status of Swirl-Flow Heat Transfer, ASME Paper 62-HT-42.
- Gambill, W.R., Bundy, R.D., and Wansborough, R.W. (1961) Heat transfer, Burnout, and Pressure Drop for Water in Swirl Flow Through Tubes With Internal Twisted Tapes, *Chemical Engineering Progress, Symposium Series No. 32*, vol. 57, pp. 127-137. (Also ORNL-2911, Apr. 1960.)
- Gambill, W.R. and Greene, N.D. (1958) Boiling Burnout With Water in Vortex Flow, *Chem. Eng. Prog.*, vol. 54, no. 10, pp. 68-76.
- Gilmour, C.H. (1958) Nucleate Boiling—A Correlation, *Chem. Eng. Prog.*, vol. 54, no. 10, pp. 77-79.
- Hersh, A.S. and Walker, B. (1980) Acoustic Behavior of Fibrous Bulk Materials, NASA Contract NAS3-21975(A80-35951), AIAA Paper 80-8096.
- Hendricks, R.C., Lattime, S., Braun, M.J. and Athavale, M.M. (1997) Experimental Visualization of Flows in Packed Beds of Spheres, *Proceedings of the First International Symposium on Flow Visualization and Image Processing*. (Also NASA TM-107365.)
- Hong, S.W. and Bergles, A.E. (1976) Augmentation of Laminar Flow Heat Transfer by Means of Twisted-Tape Inserts, *J. Heat Trans.*, vol. 98, no. 2, pp. 251-256.
- Kaviany, M. (1999) Principles of Heat Transfer in Porous Media, Second Ed., Springer-Verlag, New York.
- Koch, R. (1958) Druckverlust und Wärmeübergang bei verwirbelter Strömung. VDI-Forschungshaft 469, series B, vol. 24. (Referenced in Smithberg and Landis, 1964).
- Lopina, R.F. and Bergles, A.E. (1969) Heat Transfer and Pressure Drop in Tape-Generated Swirl Flow of Single-Phase Water, *J. Heat Trans.*, vol. 91, Aug., pp. 434-442.
- Nikuradse, J. (1933) Strömungsgesetze in rauhen Rohren, *Forschg.-Arb. Ing.-Wessen*, no. 361. (Referenced in Schlichting, 1955).
- Schlichting, H. (1955) Boundary Layer Theory, McGraw-Hill, New York.
- Silverman, L. and First, M.W. (1952) Edge and Variable Compression Filters for Aerosols, *Industrial Engineering and Chemistry*, vol. 44, no. 12, pp. 2777-2783.

- Smithberg, E. and Landis, F. (1964) Friction and Forced Convection Heat-Transfer Characteristics in Tubes With Twisted Tape Swirl Generators, *J. Heat Trans.*, vol. 86, no. 1, pp. 39–49.
- Sparrow, E.M. and Haji-Sheikh, A. (1966) Flow and Heat Transfer in Ducts of Arbitrary Shape With Arbitrary Thermal Boundary Conditions, *J. Heat Trans.*, vol. 88, series C, pp. 351–358.
- Sullivan, R.R. (1942) Specific Surface Measurements on Compact Bundles of Parallel Fibers, *J. Appl. Phys.*, vol. 13, Nov., pp. 725–730.
- Sullivan, R.R. (1941) Further Study of the Flow of Air Through Porous Media, *J. Appl. Phys.*, vol. 12, June, pp. 503–508.
- Weigand, A. (1948) The Problem of Torsion in Prismatic Members of Circular Segmental Cross Section, NACA Technical Memorandum 1182.
- Wentz, C.A. and Thodos, G. (1963) Pressure Drops in the Flow of Gases Through Packed and Distended Beds of Spherical Particles, *A.I.Ch.E. Journal*, vol. 9, no. 1, pp. 81–84.

TABLE 1.—FLOW AND PRESSURE DROP DATA AND ANALYSIS FOR 48 TWISTED TAPES IN CYLINDRICAL TUBE

\dot{V} , cm ³ /min	ΔP , psi	G_o , g/cm ² ·s	dP , g/cm·s ²	$X_{Ergun} = 0.659G_o$	$Y_{Ergun} = \frac{73.34 \times 10^{-4}}{dP/G_o^2}$	$Y_{calc} = \frac{150X_{Ergun}}{1.75} + 1.75$	Y_{calc}/Y_{Ergun}	σ_1	$X_{Ergun} Y_{Ergun}$	σ_2
^a 8218	3.55	24.33	244762	15.28	1.81	11.57	6.38	0.0039	27.69	3.42
7657	3.29	22.66	226836	14.23	1.94	12.29	6.35	0.0009	27.54	2.89
5900	2.54	17.46	175125	10.97	2.52	15.43	6.13	0.0356	27.60	3.08
4730	2.07	14.00	142720	8.79	3.19	18.81	5.90	0.1799	28.05	4.89
3881	1.67	11.49	115141	7.21	3.82	22.54	5.90	0.1797	27.58	3.03
2804	1.11	8.30	76531	5.21	4.87	30.53	6.27	0.0024	25.37	0.22
2790	1.14	8.26	78600	5.19	5.05	30.67	6.07	0.0606	26.19	0.12
1546	0.59	4.58	40679	2.87	8.51	53.95	6.34	0.0003	24.46	1.90
1272	0.47	3.77	32405	2.36	10.02	65.19	6.51	0.0353	23.68	4.65
^b 957	0.31	2.83	21374	1.78	11.67	86.07	7.37	1.1111	20.76	25.77
975	0.37	2.89	25510	1.81	13.42	84.51	6.30	0.0005	24.32	2.30
1518	0.63	4.49	43437	2.82	9.43	54.91	5.82	0.2458	26.60	0.58
2014	0.87	5.96	59984	3.74	7.40	41.82	5.65	0.4437	27.69	3.42
2713	1.13	8.03	77910	5.04	5.29	31.49	5.95	0.1377	26.70	0.74
3538	1.59	10.47	109626	6.58	4.38	24.56	5.61	0.5088	28.81	8.80
4307	1.94	12.75	133757	8.01	3.61	20.49	5.68	0.4088	28.87	9.19
5260	2.33	15.57	160647	9.78	2.90	17.09	5.89	0.1888	28.39	6.52
6129	2.67	18.14	184088	11.39	2.45	14.92	6.09	0.0548	27.92	4.34
7151	3.09	21.17	213046	13.29	2.08	13.03	6.26	0.0041	27.70	3.45
8207	3.49	24.29	240625	15.26	1.79	11.58	6.48	0.0264	27.26	2.01
6354	2.73	18.81	188225	11.81	2.33	14.45	6.20	0.0151	27.54	2.89
4435	1.92	13.13	132378	8.24	3.37	19.94	5.93	0.1557	27.75	3.65
2471	1.02	7.31	70326	4.59	5.76	34.41	5.97	0.1205	26.46	0.38
^c 1592	0.686	4.71	47298	2.96	9.33	52.44	5.62	0.4925	27.62	3.17
2721	1.174	8.05	80944	5.06	5.47	31.41	5.74	0.3320	27.66	3.30
4349	1.866	12.87	128655	8.08	3.40	20.30	5.97	0.1236	27.50	2.76
4311	1.84	12.76	126862	8.01	3.41	20.47	6.00	0.1054	27.36	2.31
6112	2.58	18.09	177883	11.36	2.38	14.95	6.28	0.0017	27.06	1.48
8045	3.37	23.81	232351	14.95	1.80	11.78	6.56	0.0581	26.85	1.02
7193	2.96	21.29	204083	13.37	1.97	12.97	6.57	0.0644	26.38	0.29
6057	2.49	17.93	171678	11.26	2.34	15.07	6.44	0.0144	26.35	0.26
4993	2.04	14.78	140652	9.28	2.82	17.91	6.35	0.0008	26.19	0.12
3459	1.41	10.24	97215	6.43	4.06	25.08	6.17	0.0221	26.13	0.08
2298	1.04	6.80	71705	4.27	6.79	36.86	5.43	0.7948	29.01	10.04
1526	0.64	4.52	44126	2.84	9.48	54.63	5.76	0.3087	26.88	1.09
958	0.39	2.84	26889	1.78	14.65	85.98	5.87	0.2045	26.09	0.06
446	0.2	1.32	13789	0.83	34.67	182.68	5.27	1.1047	28.74	8.43
^d 5859	2.52	17.34	173746	10.89	2.53	15.52	6.13	0.0353	27.57	2.99
8156	3.48	24.14	239936	15.16	1.80	11.64	6.45	0.0181	27.35	2.28
6777	2.86	20.06	197188	12.60	2.15	13.66	6.36	0.0016	27.05	1.47

^aBorda + screen (12/10/98).^bQuestionable.^cBorda + screen (12/12/98).^dBorda + screen (12/14/98).^eOrifice + screen (12/14/98; reverse of Borda + screen).^fOrifice without screen (12/14/98; reverse of Borda without screen).^gOrifice without screen (12/19/98; reverse of Borda without screen).^hN-1 points.ⁱN points.^jThrow out one point.

TABLE 1.—CONCLUDED.

\dot{V} , cm ³ /min	ΔP , psi	G_o , g/cm ² –s	dP , g/cm–s ²	$X_{Ergun} =$ $0.659G_o$	$Y_{Ergun} =$ 73.34×10^{-4} dP/G_o^2	$Y_{calc} =$ $150/X_{Ergun} +$ 1.75	Y_{calc}/Y_{Ergun}	σ_1	$X_{Ergun} Y_{Ergun}$	σ_2
4546	1.9	13.46	130999	8.45	3.17	19.50	6.15	0.0285	26.79	0.90
2367	1	7.01	68947	4.40	6.15	35.84	5.82	0.2466	27.08	1.54
1768	0.75	5.23	51710	3.29	8.27	47.39	5.73	0.3505	27.19	1.83
1245	0.55	3.69	37921	2.31	12.24	66.56	5.44	0.7740	28.32	6.13
833	0.36	2.47	24821	1.55	17.89	98.62	5.51	0.6519	27.70	3.47
718	0.32	2.13	22063	1.33	21.40	114.14	5.33	0.9753	28.57	7.44
^e 982	0.35	2.91	24131	1.83	12.52	83.92	6.71	0.1487	22.85	8.97
2239	0.88	6.63	60673	4.16	6.05	37.79	6.24	0.0059	25.19	0.42
4754	1.88	14.07	129620	8.84	2.87	18.72	6.53	0.0431	25.35	0.24
8239	3.27	24.39	225457	15.32	1.66	11.54	6.95	0.3964	25.44	0.16
7030	2.76	20.81	190294	13.07	1.93	13.23	6.87	0.3017	25.17	0.46
4265	1.65	12.62	113763	7.93	3.13	20.67	6.61	0.0832	24.80	1.09
2000	0.77	5.92	53089	3.72	6.64	42.10	6.34	0.0005	24.68	1.35
1072	0.42	3.17	28958	1.99	12.60	77.02	6.11	0.0434	25.11	0.53
722	0.28	2.14	19305	1.34	18.52	113.51	6.13	0.0366	24.86	0.96
452	0.19	1.34	13100	0.84	32.07	180.28	5.62	0.4877	26.94	1.22
^f 1297	0.47	3.84	32405	2.41	9.63	63.97	6.64	0.1020	23.23	6.82
3303	1.19	9.78	82047	6.14	3.76	26.18	6.96	0.4104	23.09	7.54
5038	1.83	14.91	126173	9.37	2.49	17.77	7.15	0.6827	23.28	6.54
6767	2.47	20.03	170299	12.58	1.86	13.67	7.35	1.0651	23.40	5.97
8412	3.08	24.90	212357	15.64	1.50	11.34	7.56	1.5308	23.47	5.62
7619	2.76	22.55	190294	14.16	1.64	12.34	7.53	1.4576	23.22	6.87
6019	2.15	17.82	148236	11.19	2.05	15.16	7.41	1.1803	22.90	8.67
4100	1.45	12.14	99973	7.62	2.97	21.43	7.21	0.7837	22.67	10.06
2003	0.704	5.93	48539	3.72	6.05	42.04	6.95	0.3935	22.53	10.96
1002	0.34	2.97	23442	1.86	11.68	82.28	7.05	0.5276	21.75	16.73
868	0.31	2.57	21374	1.61	14.19	94.72	6.68	0.1265	22.89	8.69
556	0.208	1.65	14341	1.03	23.20	146.88	6.33	0.0001	23.98	3.46
^g 1013	0.389	3.00	26820	1.88	13.07	81.41	6.23	0.0085	24.61	1.50
3095	1.17	9.16	80668	5.75	4.21	27.82	6.61	0.0817	24.23	2.59
6556	2.485	19.41	171333	12.19	1.99	14.06	7.05	0.5352	24.30	2.38
8239	3.123	24.39	215321	15.32	1.59	11.54	7.28	0.9154	24.30	2.38
5000	1.851	14.80	127621	9.29	2.55	17.89	7.01	0.4715	23.73	4.46
1700	0.621	5.03	42816	3.16	7.41	49.22	6.64	0.1039	23.42	5.88
743	0.281	2.20	19374	1.38	17.55	110.36	6.29	0.0011	24.24	2.55
					#N/A		474.00	22.56	1938.03	295.77
							6.32	0.3048	25.84	^h 4.00
								0.3007		ⁱ 3.94
										^j 3.648663

^aBorda + screen (12/10/98).^bQuestionable.^cBorda + screen (12/12/98).^dBorda + screen (12/14/98).^eOrifice + screen (12/14/98; reverse of Borda + screen).^fOrifice without screen (12/14/98; reverse of Borda without screen).^gOrifice without screen (12/19/98; reverse of Borda without screen).^hN–1 points.ⁱN points.^jThrow out one point.

TABLE 2.—TWISTED-TAPE WIDTH $\langle w \rangle$ AND THICKNESS $\langle t \rangle$ MEASUREMENTS
 FOR 48 TWISTED TAPES^a
 [Sorted in ascending order (estimated).]

Tape	Left-end measurements			Right-end measurements		
	Thickness, $\langle t \rangle$, in.	Width, $\langle w \rangle$, in.	$A = wt$, in. ²	$A = wt$, in. ²	Thickness, $\langle t \rangle$, in.	Width, $\langle w \rangle$, in.
1	0.038	0.129	0.004902	0.004514	0.037	0.122
2	.038	.124	.004712	.004674	.038	.123
3	.038	.123	.004674	.004636	.038	.122
4	.039	.122	.004758	.004674	.038	.123
5	.039	.123	.004797	.005265	.039	.135
6	.039	.125	.004875	.004797	.039	.123
7	.04	.129	.00516	.00488	.04	.122
8	.04	.124	.00496	.00492	.04	.123
9	.041	.126	.005166	.005002	.041	.122
10	.042	.118	.004956	.005453	.041	.133
11		.124	.005208	.00504	.042	.12
12		.118	.004956	.005418		.129
13		.129	.005418	.005292		.126
14		.128	.005376	.005208		.124
15		.124	.005208	.004914		.117
16	↓	.128	.005376	.005504	.043	.128
17	.043	.121	.005203	.005192	.044	.118
18	.043	.121	.005203	.00528	.044	.12
19	.043	.119	.005117	.005324	.044	.121
20	.044	.119	.005236	.005715	.045	.127
21	.047	.123	.005781	.00611	.047	.13
22	.048	.145	.00696	.0066	.05	.132
23	.049	.13	.00637	.0067	.05	.134
24	.05	.124	.0062	.0064	.05	.128
25	.051	.125	.006375	.006528	.051	.128
26	.052	.124	.006448	.0065	.052	.125
27		.128	.006656	.006916		.133
28		.123	.006396	.006552		.126
29		.126	.006552	.0065		.125
30		.125	.0065	.007182	↓	.133
31		.125	.0065	.00767	.059	.13
32		.124	.006448	.00944	.059	.16
33	↓	.125	.0065	.007847	.059	.133
34	.053	.126	.006678	.008296	.061	.136
35	.053	.125	.006625	.008235		.135
36	.054	.127	.006858	.007503		.123
37		.123	.006642	.007747	↓	.127
38		.126	.006804	.007936	.062	.128
39		.123	.006642	.008618	.062	.139
40	↓	.125	.00675	.008866	.062	.143

^aAverage porosity, 0.6105. Corresponding average t (in.) = 0.0502 and w (in.) = 0.1273.

TABLE 2.—CONCLUDED.

Tape	Left-end measurements			Right-end measurements		
	Thickness, $\langle t \rangle$, in.	Width, $\langle w \rangle$, in.	$A = wt$, in. ²	$A = wt$, in. ²	Thickness, $\langle t \rangle$, in.	Width, $\langle w \rangle$, in.
41	0.055	0.132	0.00726	0.008253	0.063	0.131
42	.055	.126	.00693	.008064	.063	.128
43	.057	.125	.007125	.009009	.063	.143
44	.061	.127	.007747	.00896	.064	.14
45	.061	.132	.008052	.00896	.064	.14
46	.062	.118	.007316	.008704	.064	.136
47	.062	.126	.007812	.00871	.065	.134
48	.065	.128	.00832	.008844	.066	.134
Totals	2.334	6.01	0.292508	0.319352	2.45	6.212
Average	0.04862	0.12521			0.05104	0.12942
Porosity			0.6276	0.5934		

^aAverage porosity, 0.6105. Corresponding average t (in.) = 0.0502 and w (in.) = 0.1273.

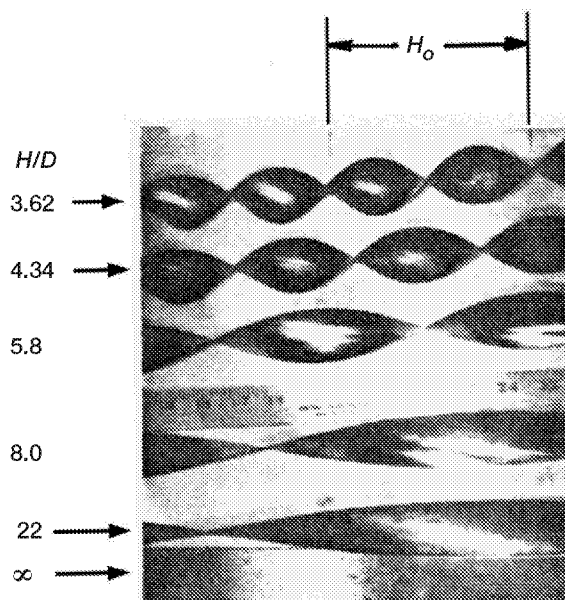


Figure 1.—Single twisted tapes. (From Smithberg and Landis, 1964.)

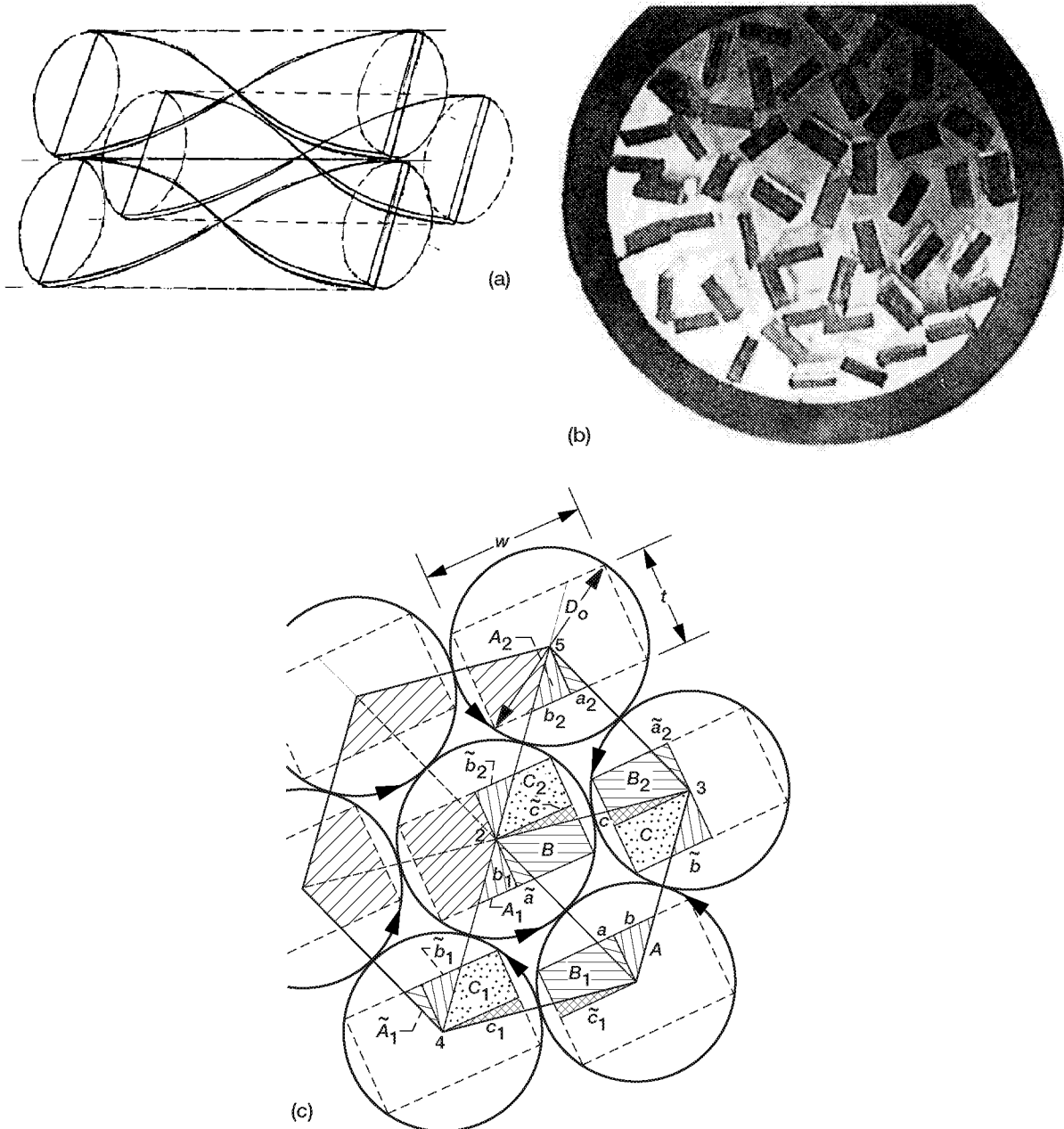
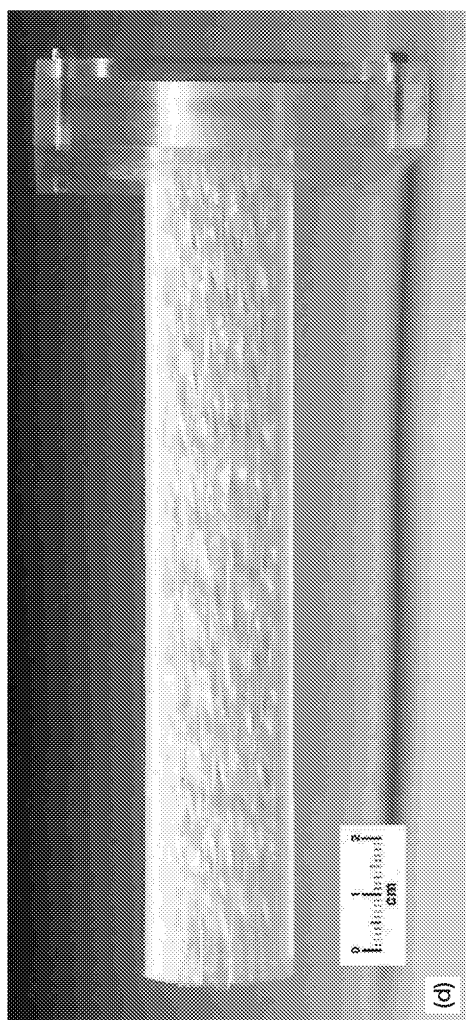
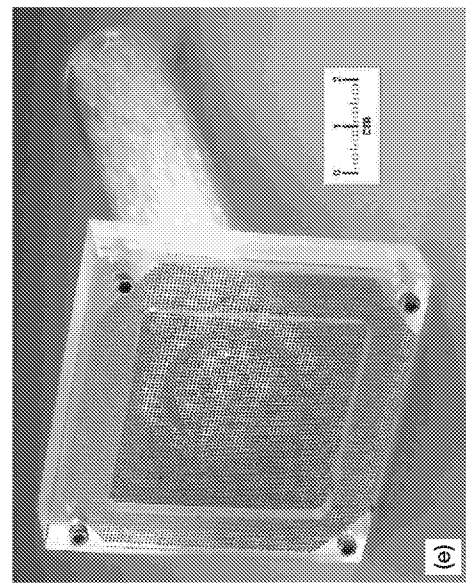


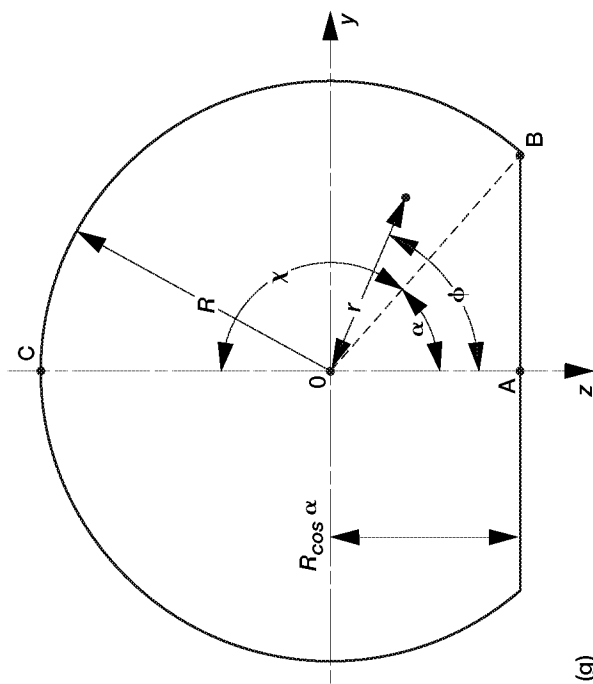
Figure 2.—Configurations of packed bed of twisted tapes. (a) Typical twisted-tape assembly. (b) Cross section (end view). (c) Ideal packed bed in soccer ball configuration. (d) Test section. (e) Test section screen. (f) Twisted tapes. (g) Prismatic bar model.



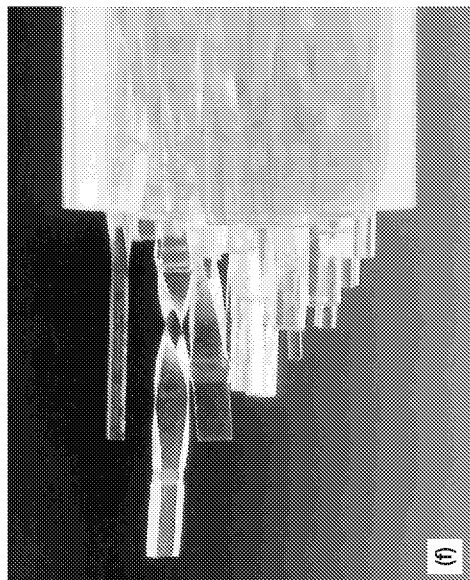
(d)



(e)



(g)



(f)

Figure 2.—(Concluded). (d) Test section. (e) Test section screen. (f) Twisted tapes. (g) Prismatic bar model.

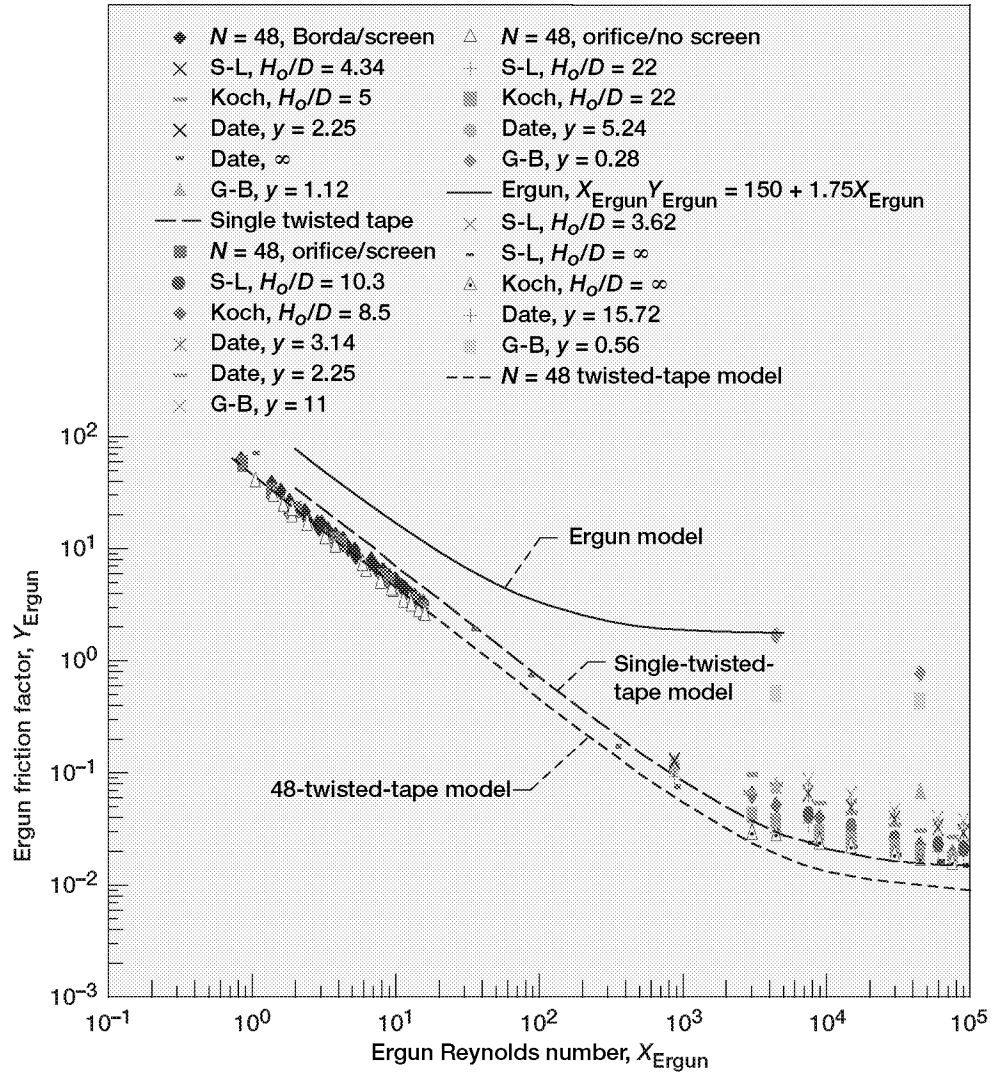


Figure 3.—Behavior for single twisted tape and 48 twisted tapes in packed bed relative to Ergun model for laminar and turbulent-flow data.

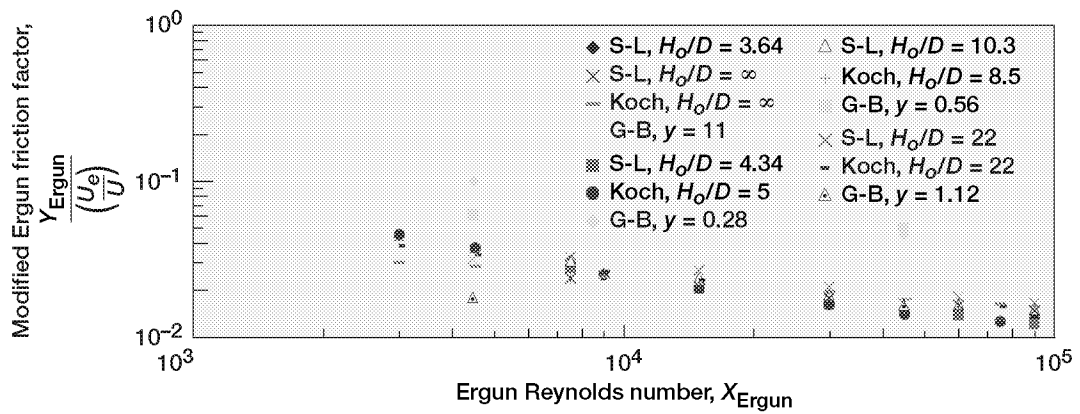


Figure 4.—Swirl velocity ratio correction (eq. (11)) applied to turbulent data.

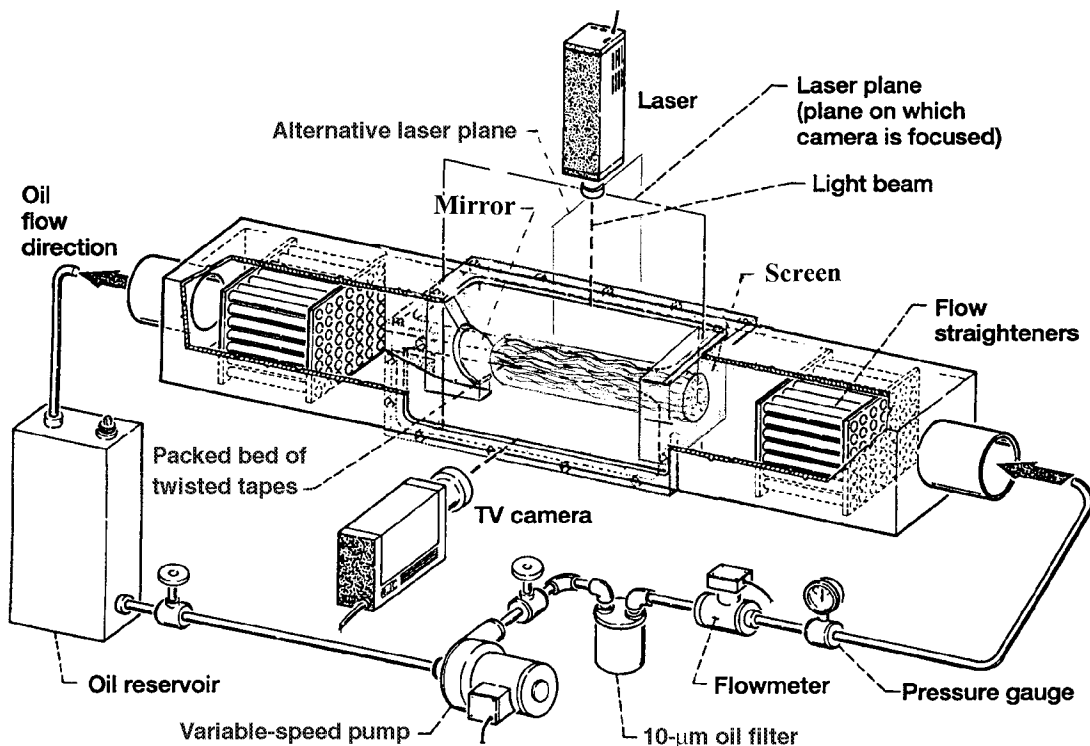


Figure 5.—Schematic of test facility.

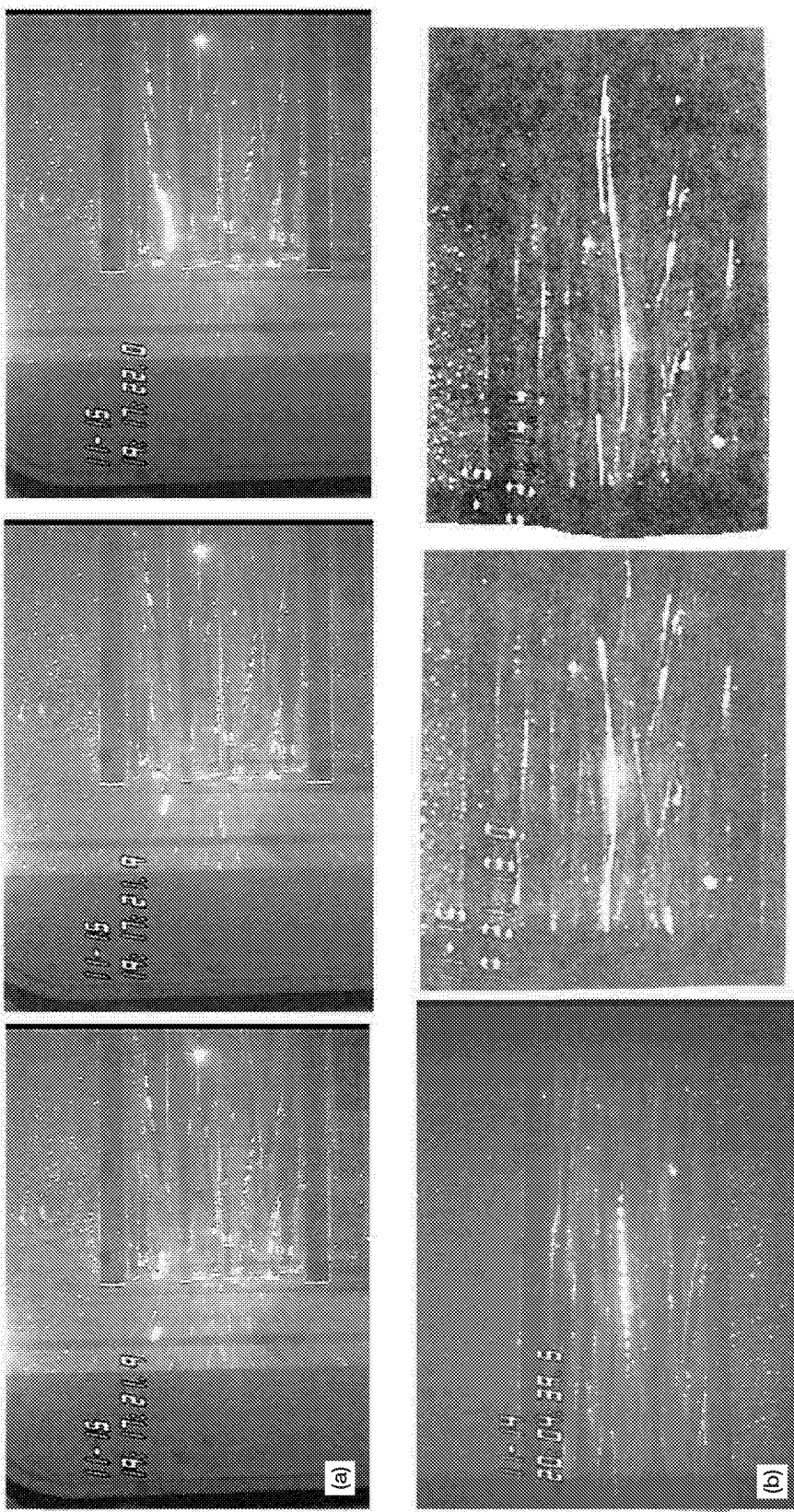


Figure 6.—Axial flow field along centerline of packed bed of twisted tapes. (a) Inlet region. (b) Developed region.

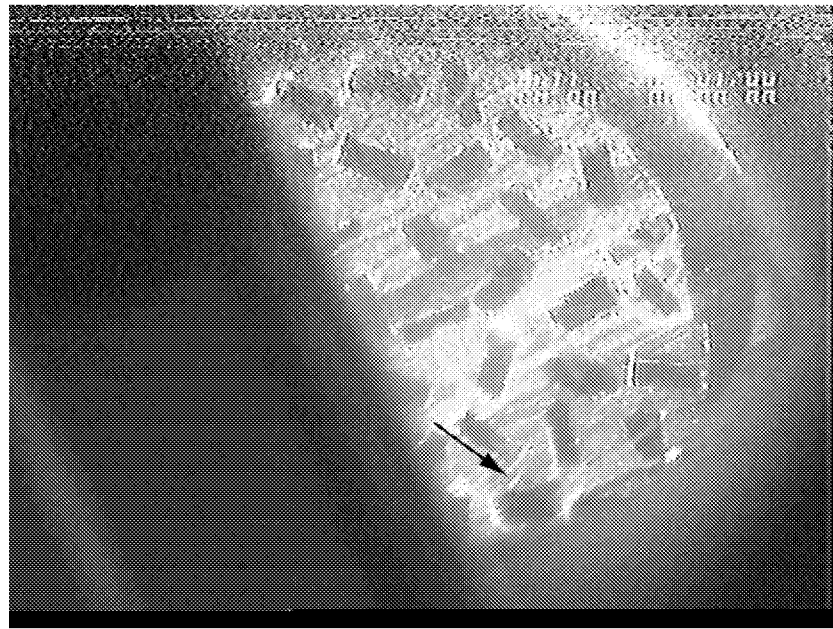


Figure 7.—Transverse flow field at one diameter from packed-bed inlet.

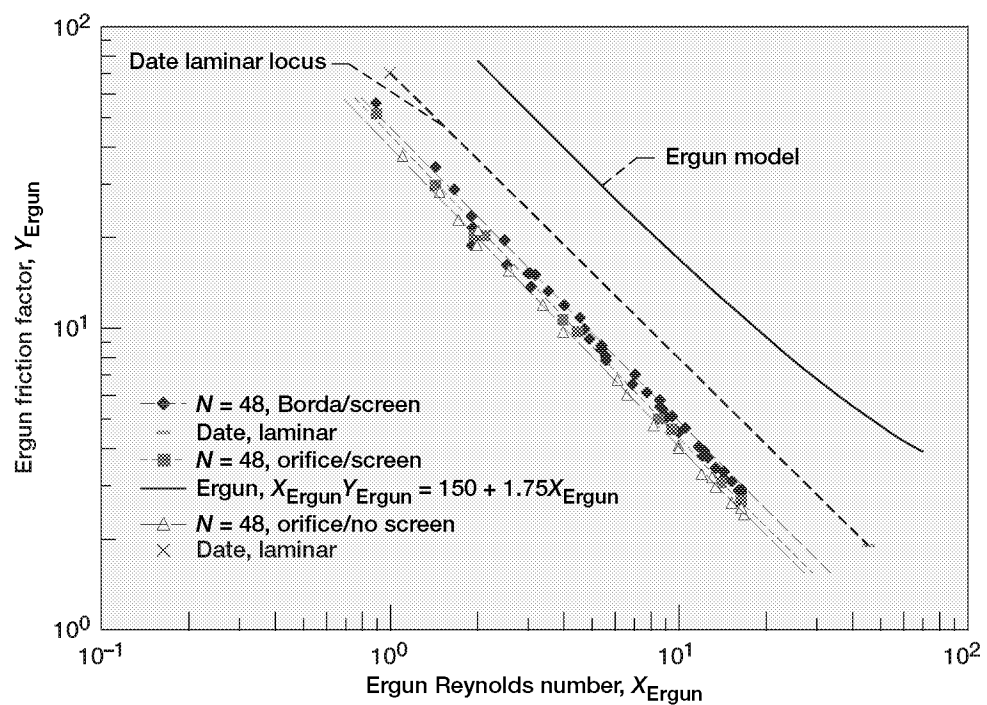


Figure 8.—Laminar flow behavior for single twisted tape and packed bed of 48 twisted tapes.

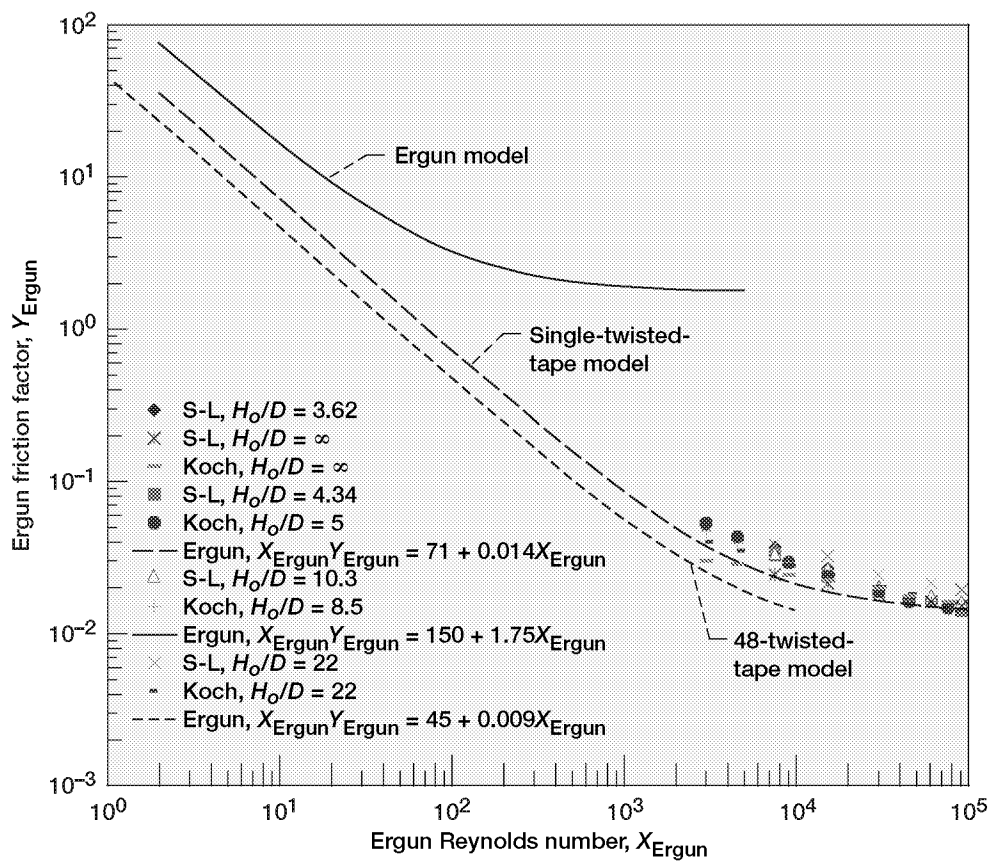


Figure 9.—Velocity-corrected turbulent data and correlation functions.

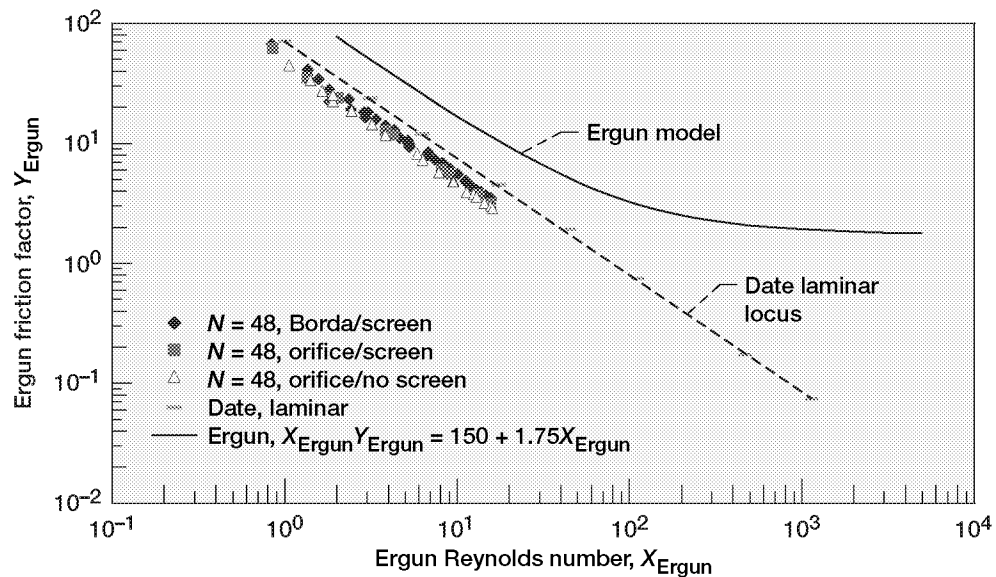


Figure 10.—Behavior of single twisted tape and packed bed of 48 twisted tapes relative to Ergun model for laminar flow data.

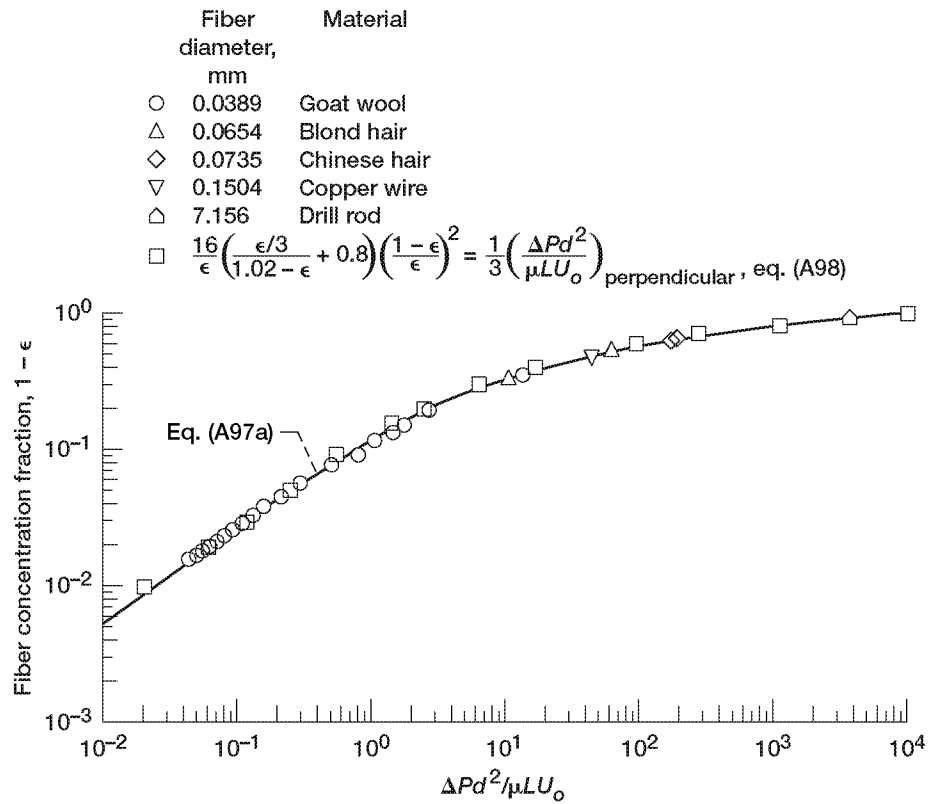


Figure 11.—Modified fit of Sullivan data (1942). (From fig. 2 of Hersh and Walker, 1980.)

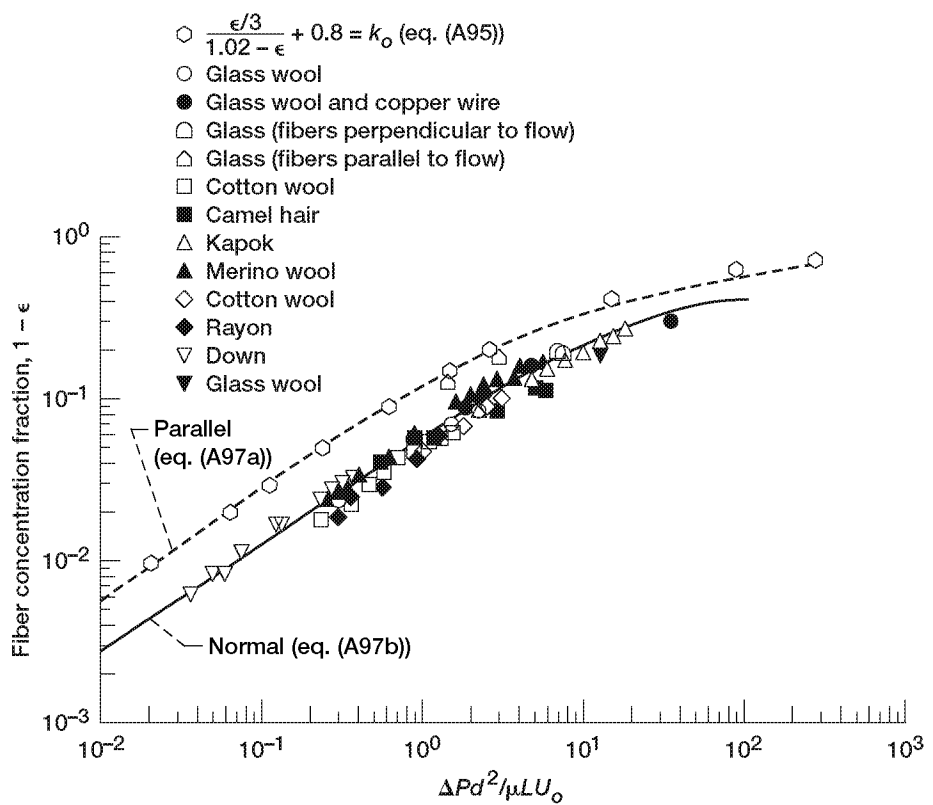


Figure 12.—Modified fit of Davies data (1952). (From fig. 3 of Hersh and Walker, 1980.)
$$\left[\frac{\Delta Pd^2}{\mu L U_o} \right]_{\text{parallel}} = \frac{16 k_o}{\epsilon} \left(\frac{1 - \epsilon}{\epsilon} \right)^2 \approx \frac{1}{3} \left[\frac{\Delta Pd^2}{\mu L U_o} \right]_{\text{normal}}$$

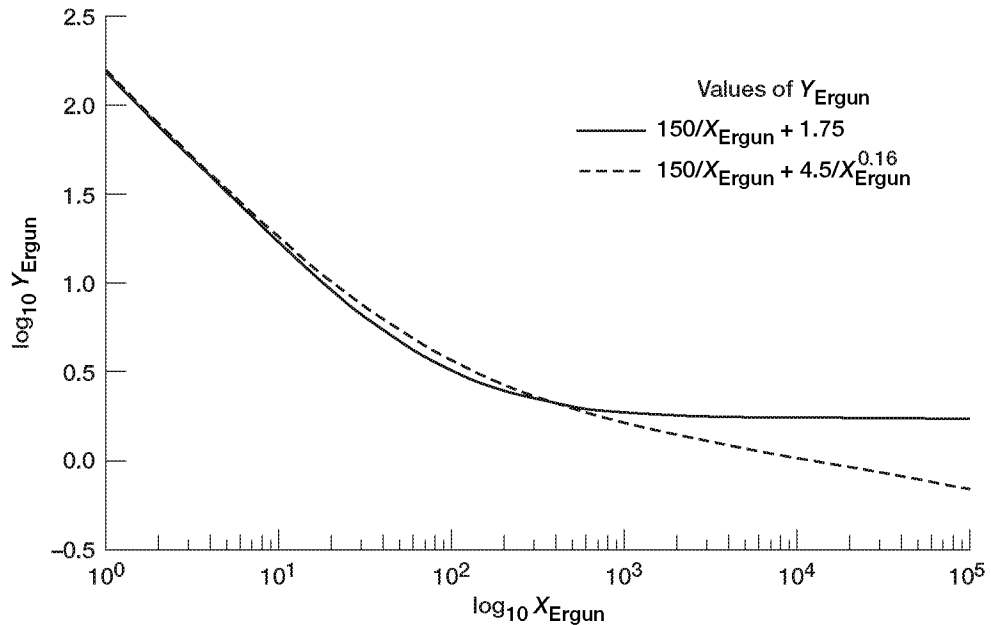


Figure 13.—Dependence of Ergun model including packed-sphere, turbulent-flow data of Wentz and Thodos (1963).

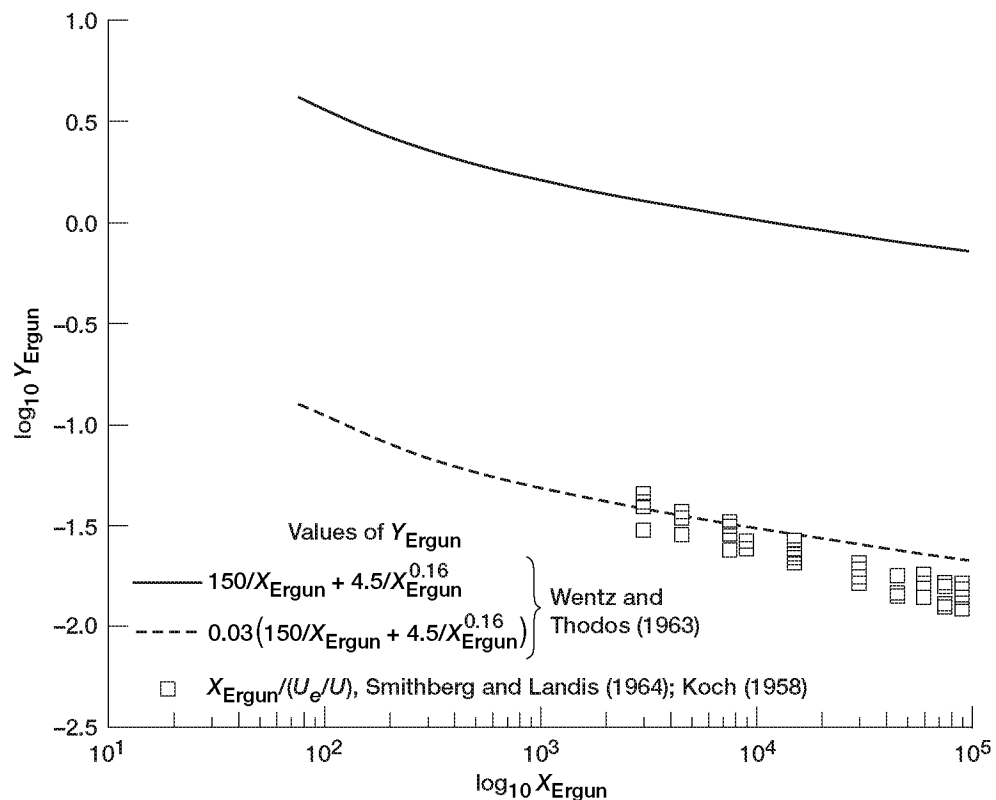


Figure 14.—Relative magnitudes and slopes of flow parameters for packed beds of spheres (Wentz and Thodos, 1963) compared with data for single twisted tape in tube (Smithberg and Landis, 1964, and Koch, 1958).

REPORT DOCUMENTATION PAGE			<i>Form Approved OMB No. 0704-0188</i>
Public reporting burden for this collection of information is estimated to average 1 hour per response, including the time for reviewing instructions, searching existing data sources, gathering and maintaining the data needed, and completing and reviewing the collection of information. Send comments regarding this burden estimate or any other aspect of this collection of information, including suggestions for reducing this burden, to Washington Headquarters Services, Directorate for Information Operations and Reports, 1215 Jefferson Davis Highway, Suite 1204, Arlington, VA 22202-4302, and to the Office of Management and Budget, Paperwork Reduction Project (0704-0188), Washington, DC 20503.			
1. AGENCY USE ONLY (Leave blank)	2. REPORT DATE	3. REPORT TYPE AND DATES COVERED	
	November 2002	Technical Memorandum	
4. TITLE AND SUBTITLE		5. FUNDING NUMBERS	
Visualization of Flows in Packed Beds of Twisted Tapes		WU-910-30-11-00	
6. AUTHOR(S)		7. PERFORMING ORGANIZATION NAME(S) AND ADDRESS(ES)	
R.C. Hendricks, M.J. Braun, D. Peloso, M.M. Athavale, and R.L. Mullen		National Aeronautics and Space Administration John H. Glenn Research Center at Lewis Field Cleveland, Ohio 44135-3191	
9. SPONSORING/MONITORING AGENCY NAME(S) AND ADDRESS(ES)		8. PERFORMING ORGANIZATION REPORT NUMBER	
National Aeronautics and Space Administration Washington, DC 20546-0001		E-11550-1	
11. SUPPLEMENTARY NOTES		10. SPONSORING/MONITORING AGENCY REPORT NUMBER	
Prepared for the Second Pacific Symposium on Flow Visualization and Image Processing sponsored by the Pacific Center of Thermal-Fluids Engineering, Honolulu, Hawaii, May 16-19, 1999. R.C. Hendricks, NASA Glenn Research Center; M.J. Braun and D. Peloso, University of Akron, Akron, Ohio 44325; M.M. Athavale, CFD Research Corporation, Huntsville, Alabama 35805; and R.L. Mullen, Case Western Reserve University, Cleveland, Ohio 44106. A supplement CD is enclosed which contains a videotape presentation of flow visualizations in a packed bed of twisted tape. Responsible person, R.C. Hendricks, organization code 5000, 216-977-7507.			
12a. DISTRIBUTION/AVAILABILITY STATEMENT		12b. DISTRIBUTION CODE	
Unclassified - Unlimited Subject Category: 34 Available electronically at http://gltrs.grc.nasa.gov This publication is available from the NASA Center for AeroSpace Information, 301-621-0390.		Distribution: Nonstandard	
13. ABSTRACT (Maximum 200 words)			
A videotape presentation of the flow field in a packed bed of 48 twisted tapes which can be simulated by very thin virtual cylinders has been assembled. The indices of refraction of the oil and the Lucite twisted tapes were closely matched, and the flow was seeded with magnesium oxide particles. Planar laser light projected the flow field in two dimensions both along and transverse to the flow axis. The flow field was three dimensional and complex to describe, yet the most prominent finding was flow threads. It appeared that axial flow spiraled along either within the confines of a virtual cylindrical boundary or within the exterior region, between the tangency points, of the virtual cylinders. Random packing and bed voids created vortices and disrupted the laminar flow but minimized the entrance effects. The flow-pressure drops in the packed bed fell below the Ergun model for porous-media flows. Single-twisted-tape results of Smithberg and Landis (1964) were used to guide the analysis. In appendix A the results of several investigators are scaled to the Ergun model. Further investigations including different geometric configurations, computational fluid dynamic (CFD) gridding, and analysis are required.			
14. SUBJECT TERMS			15. NUMBER OF PAGES 60
Flow visualization			16. PRICE CODE
17. SECURITY CLASSIFICATION OF REPORT	18. SECURITY CLASSIFICATION OF THIS PAGE	19. SECURITY CLASSIFICATION OF ABSTRACT	20. LIMITATION OF ABSTRACT
Unclassified	Unclassified	Unclassified	